

# Laser Manipulation of Atoms and Atom Optics\*

Yu-Zhu Wang and Liang Liu<sup>A</sup>

Joint Laboratory for Quantum Optics,  
Shanghai Institute of Optics and Fine Mechanics, Academia Sinica,  
P.O. Box 800-211, Shanghai 201800, China.

<sup>A</sup> Present address: Fachbereich Physik, Universität Kaiserslautern,  
Postfach 3049, D-67653 Kaiserslautern, Germany.  
e-mail: liang@physik.uni-kl.de

## *Abstract*

In this paper experiments on laser cooling, collimation and manipulation of a sodium atomic beam, such as the transverse collimation and decollimation of an atomic beam by a standing wave or a misaligned standing wave, longitudinal cooling of an atomic beam by a diffuse light field, sub-Doppler cooling in a blue detuned standing wave, are reported. The basic concept on atom optics is developed. An experiment on a method for the injection of atoms into an atomic cavity is also discussed.

## 1. Introduction

The pioneering research on the radiation force of light on free atoms and molecules was performed by Lebedev (1910) and Einstein (1916, 1917). But at that time further development of studies of light pressure was restricted by a lack of suitable light sources necessary for such investigations and this circumstance hindered not only experimental but theoretical researches as well. Thus up to 1960 only one experimental investigation (Frisch 1933) had been carried out. This investigation studied the deflection of a sodium atomic beam by sodium lamp resonance radiation. With the advent of lasers (especially tunable lasers) the radiation force of light upon free atoms was extensively studied by atomic beam deflection with a dye laser (Ashkin 1970; Schieder *et al.* 1972; Jaduszliwer *et al.* 1980; Bjorkholm *et al.* 1981; Wang *et al.* 1984a; Wang *et al.* 1985) and agreement between theory and experiment was obtained.

In 1975 two groups, Hänsch and Schawlow (1975) at Stanford University and Wineland and Dehmelt (1975) at the University of Washington, independently introduced the idea of laser cooling. In the Hänsch–Schawlow scheme, the cooling occurs because the Doppler effect introduces a velocity-dependent radiation force on the atom and therefore this kind of laser cooling is often called Doppler cooling because of the crucial role played by the Doppler effect. In the Wineland–Dehmelt scheme, the reduction in energy results from a Raman process in which transitions

\* Refereed paper based on a plenary lecture given to the joint Sixth Asia Pacific Physics Conference and Eleventh Australian Institute of Physics Congress held at Griffith University, Brisbane, July 1994.

from higher to lower kinetic energy states are more likely than the reverse. The Hänsch-Schawlow scheme is more natural when one is considering the cooling of free atoms, while the Wineland-Dehmelt scheme is more appropriate when the atoms are strongly bound in a potential well. Since that time, the investigation of laser cooling and the radiation force have become more and more exciting (Letokhov and Minogin 1981). Balykin *et al.* first reported laser longitudinal Doppler cooling of an atomic beam by scanning the laser frequency to compensate the change of Doppler shift during the cooling process (Balykin *et al.* 1979, 1980 1984*a*, 1984*b*; Balykin 1980; Andreev *et al.* 1981). Phillips and Metcalf (1982) and others (Prodan *et al.* 1982, 1985; Phillips *et al.* 1985; Migdall *et al.* 1985) achieved laser cooling of a sodium atomic beam by using a Zeeman spatial tuning magnetic field to compensate the change of Doppler shift as the atoms are slowed. By using an electro-opto modulation (EOM) technique, laser cooling of an atomic beam has also been achieved (Blatt *et al.* 1984; Ertmer *et al.* 1985). Besides the typical methods described above, several authors proposed different methods to overcome the difficulty of laser detuning due to the change of Doppler shift, such as laser cooling by diffuse light (Ketterle *et al.* 1992; Chen *et al.* 1994), laser cooling by white light (Moi 1984; Liang *et al.* 1985), and laser cooling by spatial Doppler tuning (Umezū and Shimizu 1985). Some mechanisms which do not depend on Doppler cooling have also been proposed, such as laser deceleration by the d.c. Stark effect (Breedon and Metcalf 1981) and laser cooling by the a.c. Stark effect (Wang 1980, 1981; Liu and Wang 1993; Liu *et al.* 1993).

Several authors (Gordon and Ashkin 1980; Letokhov and Minogin 1981; Castin *et al.* 1989; Lett *et al.* 1989) calculated the lowest temperature (the Doppler-cooling limit) attainable by the Doppler cooling process in the low-intensity limit and found that the thermal energy was approximately equal to the energy width of the resonant transition used for cooling. Later treatments showed that higher intensities do not yield any lower temperatures.

Atomic motion in a strong standing wave field had also been considered because of the fact that the stimulated radiation force can be much larger than the Doppler force, or spontaneous emission force. By using a continued fraction approach, the radiation force for a two-level atom in a strong standing wave field has been calculated by several authors (Letokhov *et al.* 1977; Stenholm *et al.* 1978; Minogin and Serimaa 1979; Liu and Wang 1991) and the relation between the stimulated radiation force and the transition rate has been studied in detail (Chen *et al.* 1993*a*, 1993*b*). By using a dressed-atomic approach, Dalibard and Cohen-Tannoudji (1985*a*, 1985*b*) described the motion of a two-level atom in a strong standing field and gave a physical explanation of the stimulated radiation force, which is now called the Sisyphus process. Aspect *et al.* (1986) first observed the laser cooling of atoms by a stimulated radiation force in a strong standing wave field. We have studied one-dimensional motion of slow atoms in a standing wave field (Wang *et al.* 1990) and observed the transverse velocity bunching of an atomic beam in a red-detuned standing wave field (Wang *et al.* 1994*a*).

Perhaps the most striking result in laser cooling is the realisation of a quasi-confinement of atoms within the three-dimensional, six-beam geometry envisaged by Hänsch and Schawlow (1975). The six-beam arrangement has been called optical molasses because of the viscous nature of the confinement. By extension, strong cooling accompanied by diffusive motion in one or two dimensions is called

1-D or 2-D optical molasses, respectively. Optical molasses was first observed by a group at Bell Laboratories (Chu *et al.* 1985). Two important processes for optical molasses are the real confinement of atoms in a magneto-optical trap (MOT) (Raab *et al.* 1987) and very cold trapped atoms in a vapour cell (Monroe *et al.* 1990). The first reported confinement time and temperature of the atoms were consistent with a theory based on Doppler cooling (Chu *et al.* 1985). Shortly thereafter, additional experiments brought this view into serious question. Measurements by the NIST group showed that several features of optical molasses were in strong disagreement with the theoretical predictions (Lett *et al.* 1988, 1989), and the Bell Labs group discovered an anomalously long-lived supermolasses that was not consistent with the traditional theory (Chu *et al.* 1988). Besides, the NIST group discovered that the temperature of atoms cooled by optical molasses could actually be much lower than the Doppler-cooling limit, the lowest temperature that was thought to be achievable by laser cooling. Dalibard and Cohen-Tannoudji (1989) at the Ecole Normale Supérieure in Paris and Chu and colleagues at Stanford University (Ungar *et al.* 1989; Weiss *et al.* 1989) proposed a new mechanism for laser cooling, one that relies in a fundamental way on the degeneracy of the ground state, optical pumping, and the spatial gradient of the polarisation of the cooling light. The Ecole Normale group has called this mechanism polarisation-gradient laser cooling. In this new mechanism, additional cooling is obtained but no additional diffusion appears and thus this mechanism leads to a cooling temperature well below the Doppler-cooling limit, or sub-Doppler cooling can occur.

Sub-Doppler laser cooling can also be studied in 1-D molasses. Several authors realised sub-Doppler cooling with methods different from polarisation-gradient cooling, such as laser cooling below the one-photon recoil energy by velocity-selective coherent population trapping (Aspect *et al.* 1988, 1989), atomic velocity selection using stimulated Raman transitions (Kasevich *et al.* 1991, 1992), adiabatic cooling of atoms by an intense standing wave (Chen *et al.* 1992). Sub-Doppler laser cooling in 1-D molasses has been extensively studied by the Stony Brook group (Sheehy *et al.* 1990; Shang *et al.* 1990; Straten *et al.* 1993; Padua *et al.* 1993; Gupta *et al.* 1993), such as by magnetically induced laser cooling (MILC) below the Doppler limit, velocity-selective magnetic-resonance laser cooling, transient laser cooling, bichromatic laser cooling in a three-level system and so on.

Research on the radiation force leads to the possibility of manipulating atoms by the laser field, which leads to atom optics (Mlynek *et al.* 1992; Adams *et al.* 1994; Pillet 1994). In analogy to classical optics, the field of atom optics deals with the realisation of optical elements, such as lenses (Gallatin and Gould 1991; McClelland and Scheinfein 1991; Sleator *et al.* 1992), mirrors (Cook and Hill 1982; Kasevich *et al.* 1990; Esslinger *et al.* 1993), and beam splitters for atoms (Gould *et al.* 1986; Martin *et al.* 1987; Balykin *et al.* 1993). More recently, demonstration of various types of atom interferometers have been reported, with fascinating prospects for matter-wave interferometry (Carnal and Mlynek 1991; Keith *et al.* 1991; Riehle *et al.* 1991; Kasevich and Chu 1991; Sleator *et al.* 1992). Besides, atom optics is itself a subject of much interest and a field of active fundamental research, both from an experimental and theoretical point of view. For example, consider atomic cavities in which appropriate atomic mirrors are used to trap atoms in cavities. To build such an atomic cavity, it has been

recently proposed (Balykin and Letokhov 1989) to use atomic mirrors formed by an evanescent laser wave (Cook and Hill 1982; Balykin *et al.* 1988). The cavities considered by Balykin and Letokhov (1989) are a direct duplication of cavities for light. Another kind of atomic cavity has been considered in which the use of gravity instead of one mirror of the cavity allows one to realise a cavity with only a single mirror pointing upwards (Kasevich *et al.* 1990; Wallis *et al.* 1992; Aminoff *et al.* 1993).

The description of matter wave propagation in atom optics is very similar to that in classical optics as a result of the formal analogy between the time-independent Schrödinger equation in quantum mechanics and the scalar Helmholtz equation in classical optics (Guo *et al.* 1994). Wave properties such as diffraction and interference can therefore occur when atoms are sent through microscopic mechanical structures or a light field (Carnal 1992). Different from the radiation force treatment of atomic motion in a light field, where the atoms are considered as particles, atom optics deals with the atomic motion in a light field as particle-wave propagation in the 'light medium', analogous to light wave propagation in a dielectric medium (Guo *et al.* 1994). In a light medium, the effective refractive index is described by an atomic potential energy in a light field. Thus, the analogous propagation behaviour of an atomic matter wave to a classical electromagnetic wave must satisfy the fundamental principles of classical optics, for example, focusing, reflection, refraction and etc.

This paper is arranged as follows: in Section 2, we present experimental results on the collimation and decollimation of an atomic beam in both a standing wave and a misaligned standing wave. In Section 3, we present the laser longitudinal cooling of a sodium atomic beam by a diffuse light field in an integral sphere. Section 4 describes a 1-D sub-Doppler cooling experiment in a blue detuned standing wave and gives an explanation by level-crossing and Hanle effects. In Section 5, the basic concept of atom optics is presented, and a Fabry-Perot interference filter with cold atoms is proposed. In this section, a preliminary experiment on the injection of slow atoms into atomic cavity mode is also presented. Section 6 gives the discussion and conclusion.

## 2. Atomic Motion in a Strong Standing Wave

In this section, we present basic experimental results for the motion of two-level atoms in a standing wave, such as velocity bunching, collimation and decollimation of an atomic beam in a misaligned standing wave. We first describe the apparatus used in our experiments and discuss a detection method for transverse velocity distribution developed by us, then we present our experiments and results.

### (2a) Apparatus

The apparatus used in our experiments includes two parts: the atomic beam system and the laser system. As shown in Fig. 1, the vacuum system of our atomic beam has three parts, that is the source chamber, the interaction chamber and the detection chamber. In the source chamber, a sodium oven is heated by an electrical heater automatically controlled by electronics which leads to a constant oven temperature during the experiment within  $\pm 0.5^\circ\text{C}$ . An oil diffusion pump is used in this chamber to keep the vacuum at about  $\sim 10^{-5}$  Torr. The atomic beam is produced when atoms are sprayed from the oven's nozzle with

0.5 mm diameter and is collimated by another hole with 0.5 mm diameter and 50 cm downstream from the oven. Therefore a collimated atomic beam with an original divergence angle of about  $1.5 \times 10^{-3}$  is formed in the interaction region. Since the profile of the atomic beam is a trapezium, atoms closer to the centre of the beam have lower transverse velocity. In our experiment, the most probable longitudinal velocity is about  $760 \text{ ms}^{-1}$ , which leads to a transverse velocity in the central part of the beam of less than  $0.20 \text{ ms}^{-1}$ , and on the two sides of less than  $1.14 \text{ ms}^{-1}$ , corresponding to a Doppler frequency shift of less than 2 MHz, which is one-fifth of the natural linewidth. Two turbomolecular pumps are used in both the interaction and detection chambers to keep a vacuum of  $\sim 10^{-7}$  Torr.

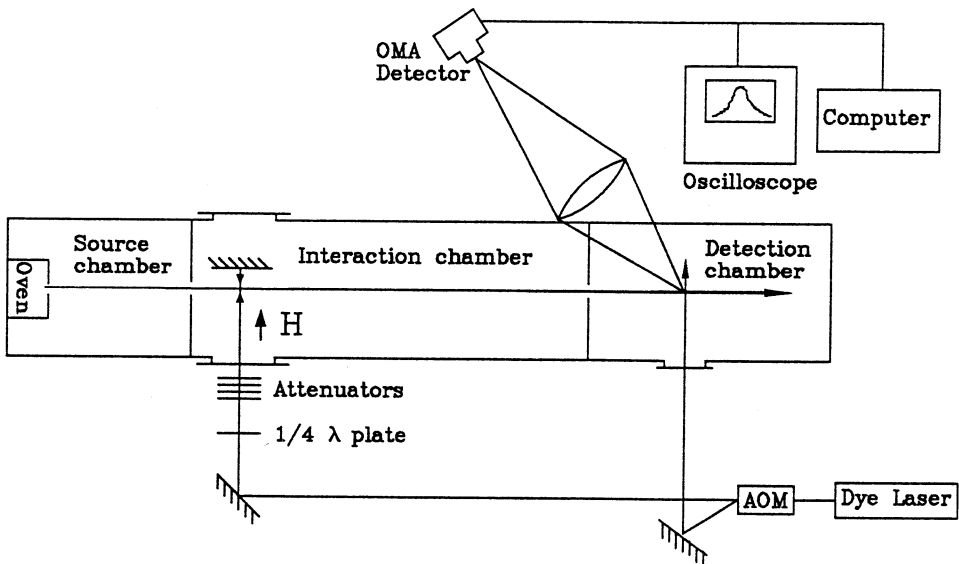


Fig. 1. Overall schematic of the apparatus used in our laboratory.

A dye laser (Coherent, Model 699-21), pumped by an  $\text{Ar}^+$  laser (Innova-200) is used to supply both interaction and detection laser light. When the laser with frequency  $\omega_L$  irradiates an acousto-optic modulator (AOM) with modulation frequency  $\Delta\omega$ , zero-order beam with frequency  $\omega_L$  and two first-order beams with frequency  $\omega_L \pm \Delta\omega$  are produced. The atomic beam is irradiated in the interaction region at right angles (along  $Oz$ ) by an intense zero-order laser beam with frequency  $\omega_L$ . The first-order beam with frequency  $\omega_L + \Delta\omega$  (or  $\omega_L - \Delta\omega$ ), tuned to be exactly resonant with the  $D_2$  line of sodium, is used to induce fluorescence of atoms in the detection region. This arrangement leads to a detuning between the laser and the atomic transition frequency in the interaction region of  $-\Delta\omega$  (or  $+\Delta\omega$ ). The detuning of the interaction laser from the atomic transition frequency can then be changed by altering the modulation frequency of the AOM.

### (2b) Transverse Velocity Detection

The final transverse velocity profile is analysed by means of the laser induced fluorescence method (LIFM) (Wang *et al.* 1984a, 1990, 1994a, 1994b) in the

detection region located 108 cm downstream from the interaction region. The basic principle of the LIFM is that when a weak laser beam irradiates the atomic beam at right angles along  $Oz$ , the atoms fluoresce with intensity proportional to the number of atoms. Therefore the spatial fluorescence intensity distribution corresponds directly to the transverse distribution of the atomic beam, from which the transverse velocity distribution can then be derived. For an atomic natural linewidth of 10 MHz (for the  $D_2$  line of the sodium atom), which is five times larger than the largest transverse Doppler shift of the initial atomic beam, as mentioned above, the LIFM is valid for atoms whose transverse velocity is less than  $5.70 \text{ ms}^{-1}$ . In our experiment, the transverse velocity is always less than this value and thus the LIFM is applicable. The spatial fluorescence distribution is imaged by a 2:1 camera lens on the detector surface of an Optical Multichannel Analyser (OMA II, Princeton Applied Research) and the intensity distribution is displayed by an oscilloscope and recorded by a computer. Some main advantages of the LIFM, compared with the hot wire method (HWM), should be mentioned, that is, high spatial resolution, rapid time response and unique detection of the atomic group corresponding to interacting atoms in the interaction region. The sensitive surface of the OMA detector, composed of a diode array with a spacing of  $25 \mu\text{m}$  between adjacent diodes, gives an excellent angular resolution of  $4.6 \times 10^{-5}$  rad for the detection system. The exposure time used in our experiments is 50 ms, which corresponds to the nearly real-time observation of the change of atomic beam profile. The unique detection by the LIFM is important especially for a ground state which has two or more hyperfine levels, for example, sodium used in our experiments has two hyperfine levels in the ground state  $3S_{1/2}$ ,  $F = 1, 2$ , as shown in Fig. 2. If the laser interacts with the atomic transition between  $3S_{1/2}$ ,  $F = 2$  and  $3P_{3/2}$ ,  $F = 3$  in sodium, the

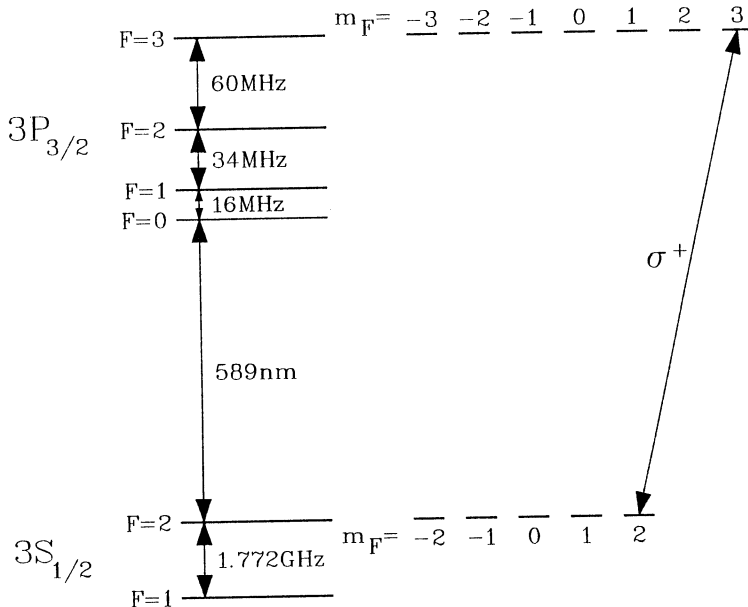
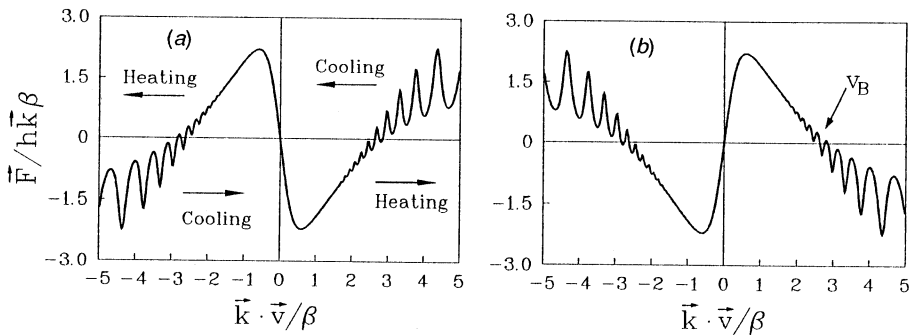


Fig. 2. Sodium energy-level diagram (not to scale). The  $\sigma^+$  polarised light field is applied to create a two-level system.

atoms  $3S_{1/2}, F = 1$  are not affected by the laser but are detected by the hot wire. Therefore, in the HWM, the 'no laser' signal must be subtracted to correct for the presence of atoms in a hyperfine level which is not interacting with the laser (Sheehy *et al.* 1990). Sometimes it is difficult to determine the number of atoms to be subtracted because it is determined not only by its thermal distribution but also by the optical pumping effect. This difficulty is automatically cancelled in the LIFM.

(2c) *Experiment on Atomic Motion in a Standing Wave*

Many authors have studied the radiation force of a two-level atom in a strong standing wave (Minogin and Serimaa 1979; Dalibard and Cohen-Tannoudji 1985; Kazantsev *et al.* 1985; Liu and Wang 1991; Chen *et al.* 1993a, 1993b). Different from the weak field or travelling field case where spontaneous emission force plays the key role, in a strong standing wave field stimulated emission becomes dominant in the interaction between atoms and lasers. The main results of the stimulated emission force for a two-level atom in a strong standing wave include: (1) laser cooling occurs for blue-detuning of the standing wave and laser heating for red-detuning, (2) the stimulated emission force does not saturate with the standing wave field intensity, and thus can be much larger than the spontaneous emission force, and (3) in a red-detuned standing wave field, the field heats slow atoms but cools fast ones, thus the two-level atoms will be bunched at a definite velocity, called the bunching velocity. The bunching velocity is determined uniquely by the detuning and intensity of the standing wave field. This phenomenon is very useful for controlling the atomic beam or scanning the atomic beam. A typical force versus atomic velocity diagram for a two-level atom in a strong standing wave is shown in Fig. 3. From Fig. 3b, we can see that atoms whose velocity is lower than a critical velocity experience a heating force and atoms whose velocity is larger than the critical value experience a cooling force. This case leads to velocity bunching. Decreasing the intensity of the standing wave to a critical intensity value, the force becomes a purely damping one. In 1990, Wang *et al.* (1990) measured this turning value which is in agreement with the theoretical result.



**Fig. 3.** Typical force-velocity curve for a two-level atom in a strong standing wave. Here the Rabi frequency is  $\Omega = 20\beta$  and (a)  $\Delta\omega = 20\beta$  and (b)  $\Delta\omega = -20\beta$ , where  $\beta$  is half the spontaneous emission rate of the excited state.

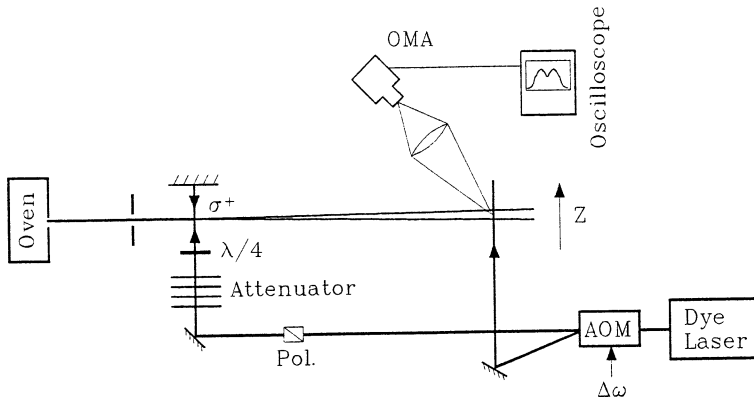


**Fig. 4.** Experimental setup for velocity bunching of two-level atoms in a red detuned strong standing wave.

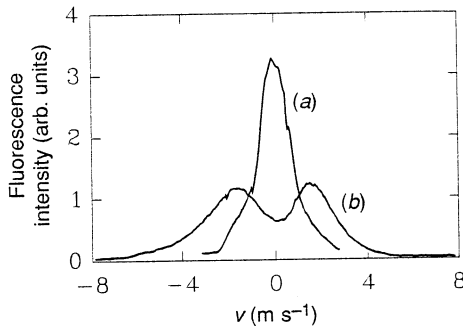


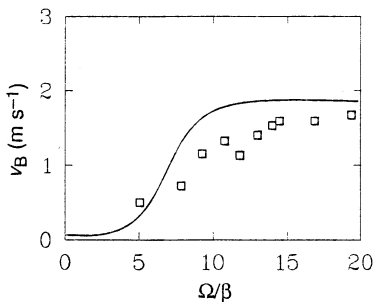
**Fig. 5.** Typical experimental result for laser cooling of two-level atoms in a red detuned strong standing wave: (a) the initial transverse velocity distribution and (b) transverse velocity bunching of atoms in a standing wave with detuning  $\Delta\omega = -5\beta$  and Rabi frequency  $\Omega = 19.4\beta$ .

Aspect *et al.* (1986) first observed laser cooling and heating of cesium atoms in a standing wave field. Here we present an experimental observation of transverse velocity bunching of a sodium atomic beam in a strong standing wave field and then report an experiment on atomic motion in a misaligned standing wave.

The experimental observation of velocity bunching has been performed with the apparatus shown in Fig. 4. A mirror is used to retroreflect the laser in order to form a standing wave. The interaction laser is tuned near the  $3S_{1/2}, F = 2 \rightarrow 3P_{3/2}, F = 3$  resonance transition and  $\sigma^+$  polarised. (A small dc magnetic field is applied along  $Oz$ .) Because of optical pumping, the atoms are rapidly locked to the transition  $3S_{1/2}, F = 2, m_F = 2 \rightarrow 3P_{3/2}, F = 3, m_F = 3$ , which achieves a two-level system (Aspect *et al.* 1986; Wang *et al.* 1994a). In the interaction region, the laser standing wave field has a Gaussian profile with a beam waist  $w = 4$  mm, which leads to a transit time of the order of  $3 \mu\text{s}$ . Fig. 5 shows a typical experimental result for laser heating or decollimation of the atomic beam interacting with a transverse standing wave with a red detuning.

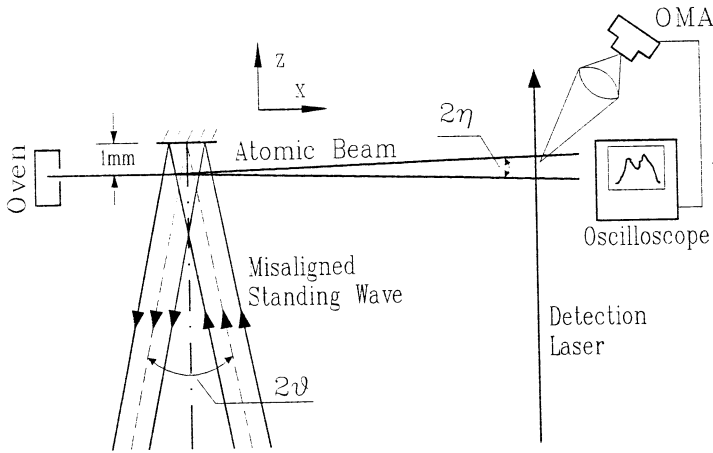
The curve (a) gives the original transverse atomic beam profile and the curve (b) gives the result of atomic beam decollimation after interaction with the standing wave field. The double-peak structure of curve (b) demonstrates the existence of velocity bunching of atoms in a standing wave field with red detuning (Wang *et al.* 1994a).

Fig. 6 gives the bunching velocity as a function of Rabi frequency with fixed detuning  $\Delta\omega = -5\beta$ . The curve shows the two-level model calculation corresponding to the experimental conditions. In the calculation, the influence of the Gaussian profile of the interaction beam is considered. The experimental results are in agreement with the two-level model calculation. This experiment also provides a test of the two-level system realised by the optical pumping method described above. As shown in Fig. 2, the excited states of the sodium atom include four hyperfine levels and in the magnetic field, every hyperfine level has magnetic sub-levels with magnetic quantum number  $m_F = -F, -F + 1, \dots, F - 1, F$ . In the experiment, the circular polarisation and the direction of the magnetic field strongly affect the realisation of a two-level system. The dependence of bunching velocity on laser power (or laser detuning) provides the possibility of scanning the atomic beam (Li 1994).



**Fig. 6.** Bunching velocity as a function of Rabi frequency with fixed detuning  $\Delta\omega = -5\beta$ . The curve gives the two-level model calculation after considering the Gaussian intensity distribution of the standing wave. The squares correspond to the experimental results. Changing the Rabi frequency leads to different bunching velocity and thus the atomic beam can be scanned.

Another possibility to realise atomic beam collimation and decollimation by the laser is to use a misaligned standing wave (DeVoe 1991) instead of a standing wave to interact with the atomic beam, as shown in Fig. 7. The misaligned standing wave is produced when a laser beam is incident upon a mirror at an oblique instead of zero angle corresponding to a standing wave. In Fig. 7, the atomic beam is irradiated in the interaction region by two travelling waves (or a misaligned standing wave) at an oblique angle  $\theta$ , called here the misalignment angle. These two travelling waves lying in the  $x-z$  plane are tilted at an angle  $\theta$  with respect to the  $z$ -axis, while the atomic beam propagates along the  $x$ -axis. The angle is defined to be positive when the projection of the propagation direction of the laser is opposite to the propagation direction of the atomic beam, otherwise  $\theta$  is negative. The collimation and decollimation of an atomic beam can be obtained only by changing the misalignment angle instead of laser intensity and detuning described above. In the experiment, the atomic beam with a most probable longitudinal velocity  $V_{mp} = 500 \text{ m s}^{-1}$  is collimated to  $\pm 1.5 \times 10^{-3}$  rad. In the interaction region, the laser misaligned standing wave has a Gaussian profile with a beam waist  $w = 6 \text{ mm}$ .



**Fig. 7.** Experimental setup used for collimation and decollimation of an atomic beam in a misaligned standing wave.

Fig. 8 compares the calculation with experimental results for an atomic beam in a misaligned standing wave with red detuning for various misalignment angles. The figure to the left gives the two-level model calculations and the other gives the corresponding experimental results. The incident laser power is 73 mW which leads to a maximum Rabi frequency of about  $9.3\beta$  and the detuning of the laser with respect to the atomic transition frequency is  $-6\beta$ . The left-hand side of Fig. 8a gives the radiation force upon atoms in a standing wave ( $\theta = 0$ ) with red detuning as a function of the divergence angle of the atomic beam. The experimental atomic beam profile detected by the LIFM after interaction of the atomic beam with a standing wave is shown on the right-hand side of this figure, which demonstrates the existence of a bunching angle (or bunching velocity) (Wang *et al.* 1994a). On the right-hand side, the central peak corresponds to the channeling of atoms in a standing wave (Salomon *et al.* 1987; Wang *et al.* 1993). The other two peaks correspond to velocity bunching of atoms. When the misalignment angle is increased to a critical value, the behaviour of the atoms in a misaligned standing wave is the same as that in a standing wave, but both the bunching angle and the maximum of the force become smaller. At the critical value of the misalignment angle, the force is nearly zero for all of the divergence angles of the atomic beam (which means for all atomic velocities), as shown in Fig. 8c. In this case, the atomic beam is spread only by momentum diffusion. The experiment gives evidence of momentum diffusion, as shown on the right side of Fig. 8c, where the atomic beam is spread but there is no bunching point. When the misalignment angle is larger than the critical one, the behaviour of the force in a misaligned standing wave is nearly opposite to that in a standing wave. The central part of the atomic beam experiences a damping force and the atomic beam whose divergence angle is larger than a critical value experiences a heating force, which results in atomic velocity bunching at zero velocity. Increasing the misalignment angle leads to an increase of the divergence-angle acceptance range of the damping force (see Figs 8d–8g). The experimental results are in agreement

with this theoretical prediction: the peak value increases when the misalignment angle is increased. But increasing the misalignment angle also leads to a decrease of the maximum force, and to capture all atoms in the divergence-angle acceptance range for larger misalignment angle, the interaction time must be longer (DeVoe 1991). For our experimental parameters, the interaction time is long enough to capture all atoms.

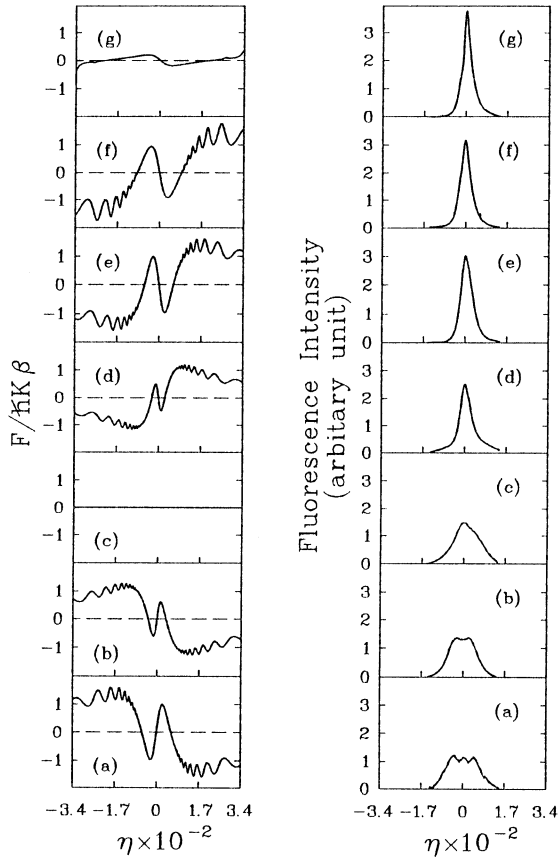


**Fig. 8.** Experimental results for collimation and decollimation of an atomic beam in a misaligned standing wave. The left-hand side gives the two-level model calculation force as a function of the divergence angle of the atomic beam  $\eta$ , and the right-hand side gives the fluorescence intensity of atoms induced by a weak resonant detection laser in the detection region as a function of divergence angle of the atomic beam  $\eta$ . Here the detuning between the laser and atomic transition frequency is  $-6\beta$  and the Rabi frequency is  $9.3\beta$ . The misalignment angle  $\theta$  is (a) 0, (b)  $2 \times 10^{-2}$ , (c)  $4 \times 10^{-2}$ , (d)  $6 \times 10^{-2}$ , (e)  $8 \times 10^{-2}$ , (f)  $1 \times 10^{-1}$  and (g)  $2 \times 10^{-1}$  rad.

The above phenomena can be understood when we consider the effective detuning experienced by an atom in a misaligned standing wave. Unlike a standing wave, in which the longitudinal velocity of the atomic beam cannot affect the detuning, in a misaligned standing wave the effective detuning is determined

not only by the laser detuning with respect to the atomic transition frequency, but also by the longitudinal velocity of the atomic beam because of the Doppler effect. From Fig. 7, we can easily determine the effective detuning for an atomic beam in a misaligned standing wave:

$$\Delta\omega_1 = \omega_L - \omega_{eg} - kv \sin(\eta - \theta), \quad (1)$$

$$\Delta\omega_2 = \omega_L - \omega_{eg} + kv \sin(\eta + \theta), \quad (2)$$

where  $\omega_{eg}$  is the atomic transition frequency and  $\eta$  is the divergence angle of the atomic beam. We know that for an atom moving in two laser fields with counter propagation directions, the atom is heated when  $(\Delta\omega_1 + \Delta\omega_2)/2 < 0$  and damped when  $(\Delta\omega_1 + \Delta\omega_2)/2 > 0$  (Liu and Wang 1991). In a misaligned standing wave, we have

$$(\Delta\omega_1 + \Delta\omega_2)/2 = \omega_L - \omega_{eg} + kv \cos \eta \sin \theta. \quad (3)$$

In a standing wave ( $\theta = 0$ ), the behaviour of the atoms is determined only by the detuning of the laser with respect to the atomic transition frequency, that is, the term  $(\Delta\omega_1 + \Delta\omega_2)/2 = \omega_L - \omega_{eg}$ , which is independent of the longitudinal Doppler shift. But in a misaligned standing wave, even though the detuning of the laser from the atomic transition frequency is red, the term  $(\Delta\omega_1 + \Delta\omega_2)/2$  can be positive when  $kv \cos \eta \sin \theta > |\omega_L - \omega_{eg}|$ . This means that, even though atoms experience a heating force in a standing wave, under the same conditions the force can become a damping one in a misaligned standing wave only by increasing the misalignment angle. Increasing the misalignment angle can also lead to an increase in the effective detuning and then to an increase in the force-acceptance range (DeVoe 1991). From the right side of Fig. 8, we find that the peak value becomes larger when the misalignment angle is increased, which means that more atoms can be damped to zero velocity for a larger misalignment angle. A special case is given in Fig. 8c, in this case,  $kv \sin \theta \approx |\omega_L - \omega_{eg}|$ , which results in zero force independent of the divergence angle of the atomic beam and the atomic beam is spread only by momentum diffusion.

Similar behaviour can also occur when the detuning between the laser field and atomic transition frequency is blue and the misalignment angle is negative, as shown in Fig. 9. In this case, the sign of the term  $(\Delta\omega_1 + \Delta\omega_2)/2$  can be changed from positive in a standing wave to negative in a misaligned standing wave when  $kv \cos \eta \sin |\theta| > |\omega_L - \omega_{eg}|$ , where  $\theta$  must be negative.

In conclusion, we have studied atomic motion in a standing wave and in a misaligned standing wave with both red and blue detuning for different misalignment angles and observed collimation and decollimation of an atomic beam in a standing wave or in a misaligned standing wave. By using these results, we can control or scan an atomic beam by changing the detuning, intensity and misalignment angle. The atomic beam can be more exactly controlled when it is monochromatic. Our results are useful for the cooling of an atomic beam by the stimulated force. In fact, a misaligned standing wave consists of a standing wave along the  $z$ -axis with wavelength of  $\lambda/\cos \theta$  which is much larger than that of a standing wave. This long wavelength increases the region of linear velocity damping from  $2\beta$  to  $20 \rightarrow 40\beta$  so that a substantial fraction of

a Doppler-broadened atomic beam can be cooled simultaneously. This method makes it easy to cool longitudinal atomic beams (DeVoe 1991).

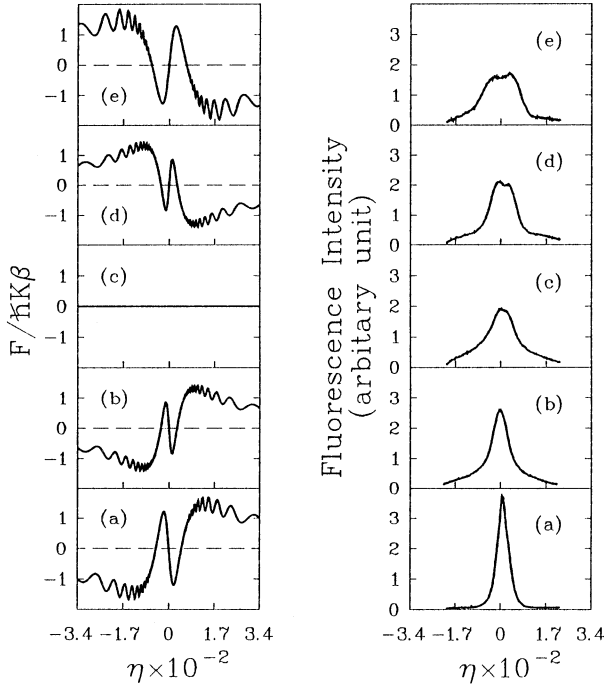


**Fig. 9.** Same as Fig. 8, but here the detuning is  $+6\beta$  and the Rabi frequency is  $10.97\beta$ . The misalignment angle  $\theta$  is (a) 0, (b)  $-1 \times 10^{-2}$ , (c)  $-3 \times 10^{-2}$ , (d)  $-5 \times 10^{-2}$ , and (e)  $-7 \times 10^{-2}$  rad.

### 3. Laser Cooling by a Diffuse Light Field

Laser cooling of an atomic beam was first achieved by using single-mode lasers by either chirping the frequency (Blatt *et al.* 1984; Ertmer *et al.* 1985) or tuning the atomic resonance in an inhomogeneous magnetic field (Phillips and Metcalf 1982; Prodan *et al.* 1982). A third possibility consists of the utilisation of non-monochromatic radiation. Zueva and Minogin (1981) showed that an increase in the number of the laser modes may improve the cooling rate as a consequence of the larger number of atoms in resonance with the field. Moi (1984) suggested a method of achieving laser cooling by using a broadband laser. By using a mode-locked laser, Strohmeier *et al.* (1989) observed a beam deceleration. Zhu *et al.* (1991) reported the first observation of atomic cooling by using both a broadband laser and a co-propagating single mode laser beam, as suggested by Hoffnagle (1988). This second laser is necessary for compensating the residual cooling generated by the tail of the laser spectrum on the atoms brought to rest. Liang *et al.* (1984) and Gozzini *et al.* (1991) observed atomic deceleration by using only the 'lamp-laser'. Ketterle *et al.* (1992) reported an experiment on slowing atoms in an isotropic light field and Batelaan *et al.* (1994) achieved laser cooling of Rb atoms with isotropic light.

In non-monochromatic radiation cooling, the power per mode is an important parameter in the cooling process. The low power per mode limits the the cooling efficiency. Here we report a laser cooling experiment using a diffuse light field. The diffuse light field is produced by a laser beam incident in an optical integral sphere cavity, which can enhance the power per mode by  $Q$ . The intensity of the diffuse light in the cavity is then

$$I = PQ, \quad (4)$$

$$Q = \frac{4\rho}{\pi d^2(1-\rho)}, \quad (5)$$

where  $P$  is the power of the incident laser beam,  $\rho$  is the reflectivity coefficient, and  $d$  is the diameter of the integral sphere. If  $\rho$  is approximately 99%, the intensity of diffuse light field is enhanced by two orders and thus the power requirement for laser cooling is reduced.

The basic principle for laser cooling in a diffuse light field is the use of an angle-dependent Doppler shift to compensate the Doppler shift change during the cooling process. If a light field with frequency  $\omega_L$  propagating at an angle  $\theta$  with respect to the propagation direction of an atomic beam moving with velocity  $v$ , then due to the Doppler effect, the effective frequency experienced by the atoms is

$$\omega = \omega_L \left( 1 + \frac{v}{c} \cos \theta \right), \quad (6)$$

where  $c$  is the speed of light. It is on resonance when  $\omega_{eg} = \omega$ , that is

$$\omega_{eg} = \omega_L \left( 1 + \frac{v}{c} \cos \theta \right). \quad (7)$$

From equation (7), the resonance condition can be satisfied by changing the angle  $\theta$ , instead of chirping the laser frequency  $\omega_L$  (Balykin *et al.* 1979; Blatt *et al.* 1984) or by tuning the atomic resonance transition frequency  $\omega_{eg}$  (Phillips and Metcalf 1982), when  $v$  is changed during the cooling process. The diffuse light field in an optical integral cavity can supply light at all directions and thus the compensation for the Doppler shift change due to the change of atomic velocity during the cooling process in a diffuse light field can be automatically obtained. Different from the cooling by a broadband laser, in which it is necessary to add a single mode co-propagating laser to compensate the residual cooling generated by the tail of the laser spectrum on the atoms, in a diffuse light field with red detuning, the atoms can be cooled to the lowest velocity when  $\theta = 0$ ,

$$kv_{\text{lowest}} = \omega_{eg} - \omega_L, \quad (8)$$

where  $k$  is the wave vector. The lowest velocity for cooling is determined only by the detuning between the laser frequency and the atomic transition frequency. For atoms whose velocity is lower than the lowest velocity, the diffuse light field has no effect because of the off-resonance. Thus the diffuse light field can

decelerate the high-speed atoms over a wide range to the lowest velocity given by equation (8) and then the decelerating process is stopped. In the end, the atomic beam is monochromatic and laser cooling can be realised. From equation (8), we find that a different detuning leads to a different final cooling velocity.

A simple calculation of the radiation force on a two-level atom in a diffuse light field can help us to understand the cooling process. If we consider a travelling wave whose propagation direction has an oblique angle  $\theta$  with respect to the atomic beam, the spontaneous emission force is (Letokhov and Minogin 1981)

$$F(\theta) = \hbar k \beta \frac{G}{1 + G + (\Delta\omega + kv \cos \theta)^2 / \beta^2}, \quad (9)$$

where  $\Delta\omega = \omega_L - \omega_{eg}$ ,  $G = I/I_s$  is the saturation parameter,  $I_s$  is the saturation intensity ( $I_s = 6$  mW for the  $D_2$  line in sodium) and  $I$  is the energy density of the diffuse light field. In the diffuse light field, the radiation force for a definite velocity can be obtained by an integral over frequency space (Doppler shift) (Hoffnagle 1988)

$$F = \int B kv F(\theta) \sin 2\theta d\theta, \quad (10)$$

where  $B$  is a normalising constant. From equations (9) and (10), we have the spontaneous emission force for a two-level atom in a diffuse light field

$$F = -\frac{\hbar k \beta G}{2\pi} \left[ \frac{\beta C}{2kv} + \frac{\Delta\omega D}{kv} \right], \quad (11)$$

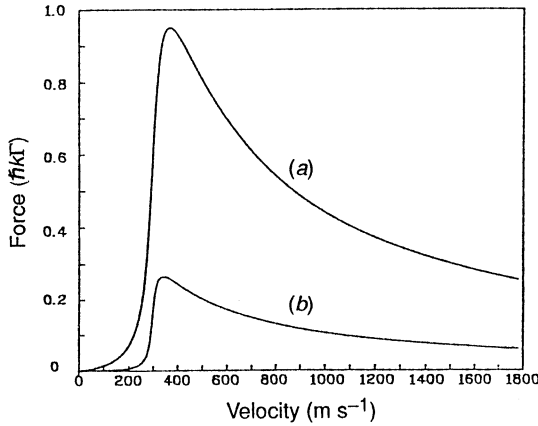
where

$$C = \ln \frac{(1 + G)\beta^2 + \Delta\omega^2}{(1 + G)\beta^2 + (\Delta\omega + kv)^2}, \quad (12)$$

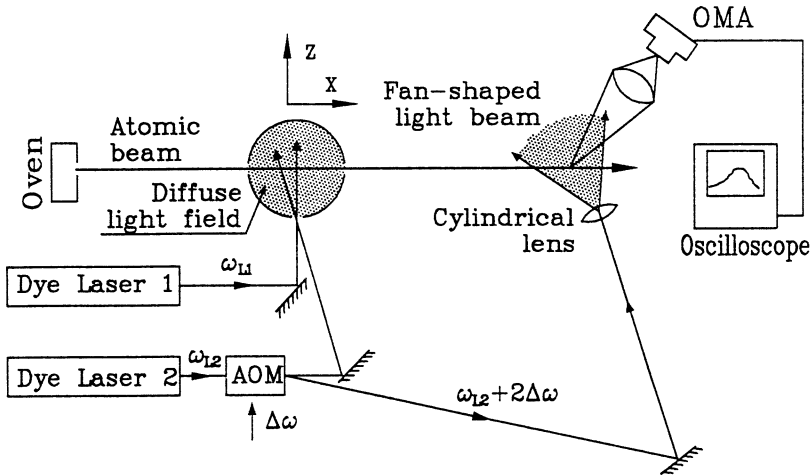
$$D = -\frac{1}{\sqrt{1 + G}} \left[ \tan^{-1} \frac{\Delta\omega}{\beta\sqrt{1 + G}} - \tan^{-1} \frac{\Delta\omega + kv}{\beta\sqrt{1 + G}} \right]. \quad (13)$$

Fig. 10 gives a typical numerical calculation for two different saturation parameters. The radiation force has a wide velocity range; for example, for the case given in Fig. 10, from 300 to 1200  $\text{ms}^{-1}$  the radiation force remains large enough for cooling.

The experimental scheme for longitudinal cooling of a sodium atomic beam in a diffuse light field is shown in Fig. 11. A laser beam detuned by  $\Delta\omega_1$  with respect to the transition frequency  $3S_{1/2}, F = 2 \rightarrow 3P_{3/2}, F = 3$  of the sodium  $D_2$  line is incident in an optical integral sphere with diameter of 50 mm to form a diffuse light field for cooling. Another laser, or repumping laser, detuned by  $\Delta\omega_2$  with respect to the atomic transition between  $3S_{1/2}, F = 1$  and  $3P_{3/2}, F = 2$  is simultaneously incident in the sphere to eliminate optical pumping. We use the zero order beam from an AOM with a modulation frequency  $\Delta\omega$ , irradiated by a laser with frequency  $\omega_{L2}$ , as the repumping beam and a second order beam with a frequency  $\omega_{L2} + 2\Delta\omega$  to detect the longitudinal velocity distribution of the



**Fig. 10.** Resonance radiation force versus velocity for two saturation parameters in a diffuse light field with detuning  $-650$  MHz: (a)  $G = 10$  and (b)  $G = 1$ .



**Fig. 11.** Experimental setup used for laser longitudinal cooling of an atomic beam in diffuse light fields. Two laser beams are incident in the integral sphere to avoid optical pumping.

atomic beam before and after cooling. The velocity distribution is analysed by a spatial fluorescence technique (Wang *et al.* 1984*b*; Chen *et al.* 1992*b*), similar to the LIFM described in Section 2. A divergent, fan-shaped laser beam, formed by the second order light beam with frequency  $\omega_{L2} + 2\Delta\omega$  passing through a cylindrical lens, interacts with the atomic beam in the detection region. When an atom with resonant transition frequency  $\omega_{eg}$  moves with velocity  $v$  along the  $x$ -axis, due to the Doppler effect, the resonant condition is

$$\omega_{eg} = (\omega_{L2} + 2\Delta\omega) \left( 1 - \frac{v}{c} \cos \theta' \right) \quad (14)$$

or

$$\cos \theta' = \frac{\Delta\omega_2 + 2\Delta\omega}{k_2 v}, \quad (15)$$

where  $k_2 = (\omega_{L2} + 2\Delta\omega)/c$ . Equation (15) implies that a different velocity in the atomic beam corresponds to a different resonant incident angle  $\theta'$  in the fan-shaped laser beam or, in other words, an atom with a different velocity, excited by a fan-shaped laser beam, fluoresces at a different position along the  $x$ -axis. Thus the longitudinal velocity distribution of the atomic beam can be obtained by measuring the spatial fluorescence distribution along the  $x$ -axis (Wang *et al.* 1984*b*; Chen *et al.* 1992). In the experiment, the detuning for both of the two laser beams incident in the sphere is  $\Delta\omega_1 = \Delta\omega_2 = -650$  MHz and the saturation parameter  $G_{L1} = G_{L2} = 3.1$ . The temperature of the sodium oven is 515 K. Because of the limit of our probe condition, only the atoms with velocity less than  $750 \text{ m s}^{-1}$  can be analysed. Fig. 12 gives typical experimental results for longitudinal cooling of an sodium atomic beam in a diffuse light field. Fig. 12*a* corresponds to the initial velocity distribution of the atomic beam and in Fig. 12*b*, when the diffuse light field is on, a small peak appears which demonstrates the longitudinal cooling. The peak has a velocity of about  $380 \text{ m s}^{-1}$  and a width about  $20 \text{ m s}^{-1}$ .

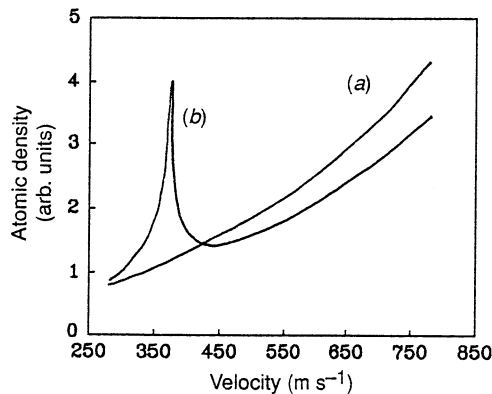


**Fig. 12.** Typical experimental results for laser cooling in a diffuse light field: (a) initial longitudinal velocity distribution of an atomic beam, and (b) cooled longitudinal velocity distribution, where a small peak appears at velocity  $380 \text{ m s}^{-1}$  with width about  $20 \text{ m s}^{-1}$ . Both curves are smoothed.

In conclusion, we have studied longitudinal cooling of an atomic beam in a red-shifted diffuse light field, formed in a optical integral sphere injected by a laser light. We have observed the cooling of atoms to  $380 \text{ m s}^{-1}$  with velocity width  $20 \text{ m s}^{-1}$ . In the red-shifted diffuse light cooling, since the final velocity is determined by the laser frequency and the atomic density in the peak is determined by the interaction distance, two or more optical integral sphere cavities injected by different light with appropriate frequencies are useful in the experiment for increasing the cooling velocity range over the interaction distance. In this case,

all of the atoms can be decelerated to a definite velocity which can be very close to zero velocity. Since the diffuse light field cooling in an integral sphere is efficient over a large velocity range, high density optical molasses can be formed in an optical integral sphere with an appropriate arrangement. Therefore, it is very interesting to consider diffuse light field cooling in an absorption cell.

#### 4. Sub-Doppler Laser Cooling in a Blue-detuned Standing Wave

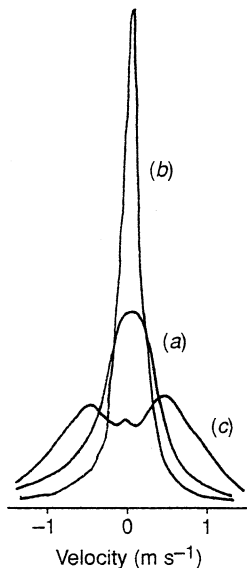
In this section, we describe a sub-Doppler laser cooling experiment. The experimental arrangement is similar to those described in Section 2 (Aspect *et al.* 1986; Wang *et al.* 1994) and MILC (Sheehy *et al.* 1990). But in our experiment, the sub-Doppler cooling is observed in a blue-detuned standing wave instead of a red one in MILC. We attribute the cooling process to level crossing and Hanle effects. In this section, we first present the sub-Doppler laser cooling experiments and then give an explanation of the experimental results by using the Sisyphus process.

##### (4a) Experiment

The experimental scheme for sub-Doppler laser cooling in a blue-detuned standing wave is the same as that described in Section 2 (Aspect *et al.* 1986; Wang *et al.* 1994a, 1989) and MILC (Sheehy *et al.* 1990; Shang *et al.* 1990) except for the direction of the magnetic field. In Section 2, the direction of the magnetic field is exactly parallel to the propagation direction of the standing wave in order to achieve a two-level system, and in MILC, the direction of magnetic field is perpendicular to the propagation direction of the standing wave in order for the magnetic field to mix the different light-shifted atomic ground-state sublevels. The lowest obtainable temperature for optical cooling of two-level atoms in a standing wave is the Doppler temperature (Wineland and Itano 1979)  $T_D = \hbar\beta/2k_B$  ( $\sim 240 \mu\text{K}$  for sodium), where  $k_B$  is the Boltzmann constant. In MILC, the sub-Doppler cooling can be achieved by using a standing wave with uniform polarisation and a transverse magnetic field. This process can be described by the Sisyphus effect (Dalibard *et al.* 1985a, b), that is, when the laser is tuned below resonance, atoms travelling across the standing wave will be optically pumped to the lowest energy sublevel near an antinode, and redistributed among the higher sublevels near a node by Larmor precession. Travel across the next antinode repeats the process and extracts energy from the atoms, thereby damping their motion. In our sub-Doppler cooling, besides the magnetic field parallel to the propagation direction of the standing wave, another magnetic field is applied which is perpendicular to the propagation direction of the standing wave and much weaker than the parallel magnetic field. The role of the parallel magnetic field is to remove the degeneracy of the atomic ground-state sublevels so that the sublevels cross at some points in a strong standing wave due to the a.c. Stark effect. The perpendicular magnetic field then mixes the sublevels. When the laser is detuned to the blue, atoms travelling across the standing wave will be optically pumped to the lowest energy sublevel near a node, and redistributed among the higher sublevels near a crossing point by Larmor precession. Travel across the node repeats the process and extracts energy from the atoms, so that sub-Doppler cooling occurs in a blue-detuned standing wave.

The experimental conditions are as follows: The divergence angle of the atomic beam is  $1.5 \times 10^{-3}$  rad. The most probable longitudinal velocity is about  $760 \text{ ms}^{-1}$ . The diameter of the standing wave is  $4.5 \text{ mm}$ , which leads to an interaction time of  $5.9 \times 10^{-6} \text{ s}$ , much longer than the lifetime of the excited state. The final transverse velocity distribution is analysed by the LIFM.

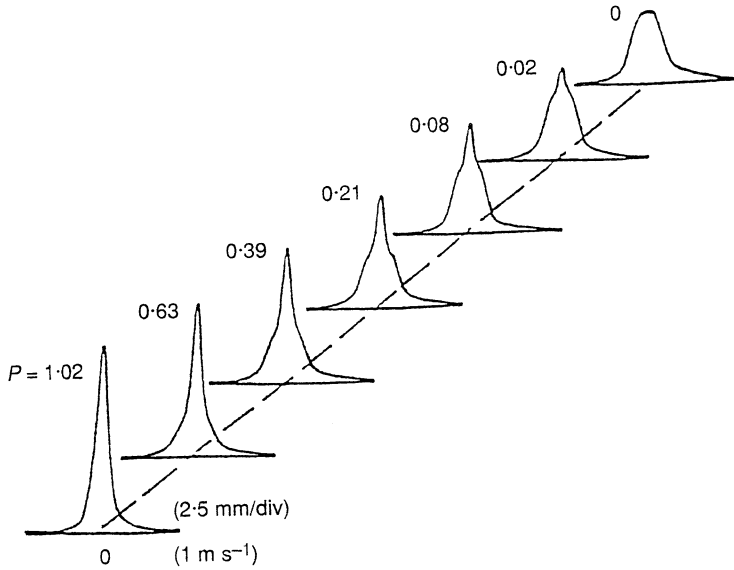
Typical experimental results for sub-Doppler transverse laser cooling of an atomic beam in a blue-detuned standing wave are shown in Fig. 13. The standing wave is  $\sigma^-$  polarised (the polarisation of the standing wave is important for sub-Doppler cooling, as shown the in following). The laser power used in the experiment is  $110 \text{ mW}$ , which leads to a saturation parameter  $G = 108$  or  $P = G/[(\Delta\omega/\beta)^2 + 1] = 1.02$ , where the detuning is  $\Delta\omega = 50 \text{ MHz}$ . The original atomic beam, shown in Fig. 13a, has a transverse velocity  $0.57 \text{ ms}^{-1}$ , which corresponds to a transverse temperature  $274 \mu\text{K}$ . Fig. 13b gives the sub-Doppler cooling result of  $0.15 \text{ ms}^{-1}$  transverse velocity, which corresponds to  $60 \mu\text{K}$ , much lower than the Doppler limit  $240 \mu\text{K}$ .



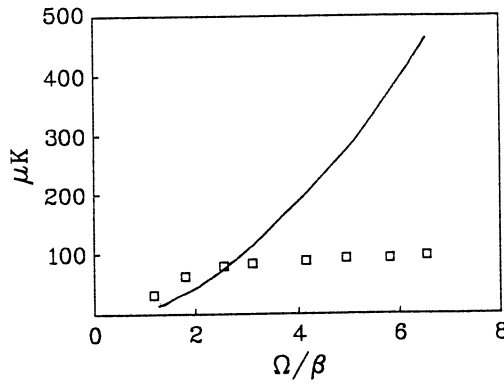
**Fig. 13.** Typical sub-Doppler cooling results in a blue-detuned standing wave with  $\sigma^-$  polarisation: (a) laser beam off, (b) laser beam on with detuning  $\Delta\omega = 10\beta$ , and (c) laser beam on with detuning  $\Delta\omega = -4.4\beta$ .

Fig. 14 gives the dependence of sub-Doppler laser cooling on the saturation parameter of the standing wave with detuning  $+50 \text{ MHz}$ . When the saturation parameter is decreased, a 'shoulder' of  $0.8 \text{ mm}$  width appears at the central part of the atomic beam profile. The width is just equal to the diameters of the collimation hole of the atomic beam. This case means that there is a potential which can trap the atoms and, during motion in the potential, the atoms are cooled. Outside the potential, the atoms with velocity higher than the trapping velocity of the potential cannot be cooled by the sub-Doppler cooling force. Fig. 15 gives a comparison between the sub-Doppler cooled and the trapped temperature in a standing wave potential. The curve in Fig. 15 shows the trapped temperature of a standing wave potential (Ashkin 1978; Salomon *et al.* 1987)

$$U(x) = \frac{1}{2} \hbar \Delta\omega \ln \left[ 1 + \frac{\Omega^2(x)}{2(\Delta\omega^2 + \beta^2)} \right], \quad (16)$$



**Fig. 14.** Transverse velocity distribution of sub-Doppler cooling in a blue-detuned standing wave with  $\sigma^-$  polarisation for various saturation parameters.



**Fig. 15.** Sub-Doppler cooling temperature in a  $\sigma^-$  polarised standing wave with detuning  $\omega = 10\beta$ , as a function of the relative Rabi frequency  $\Omega/\beta$ . The curve shows the trapped temperature for atoms in the potential well of a standing wave.

as a function of saturation parameter. As the saturation parameter increases, the potential becomes large and the velocity at which the potential can trap becomes larger. The sub-Doppler cooling experimental results, given as squares in Fig. 15, show that the cooling temperature remains constant, about  $100 \mu\text{K}$ , when the saturation parameter is increased.

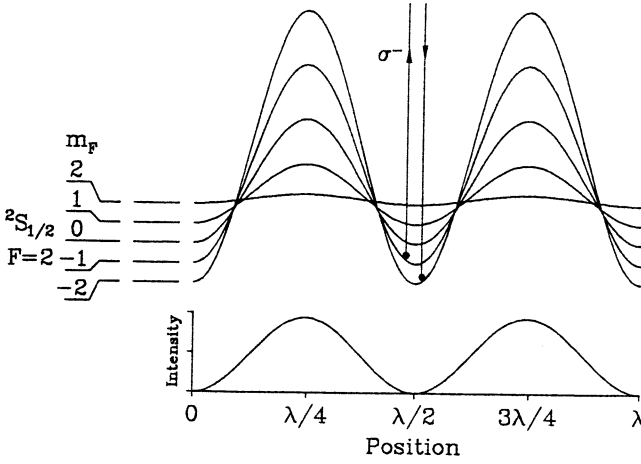


**Fig. 16.** Sisyphus process for an atom in a blue-detuned standing wave with  $\sigma^-$  polarisation. The left-hand side gives the Zeeman splitting of the sodium  $3S_{1/2}, F = 2$  state, and the right-hand side gives the total shift of the energy levels in a magnetic field and a laser standing wave. The bottom curve corresponds to the spatial intensity dependence of the standing wave.

*(4b) Sisyphus Process of Sub-Doppler Laser Cooling*

In this subsection, we develop a Sisyphus model to explain the above sub-Doppler cooling results in a blue-detuned standing wave. The Zeeman splitting occurs because of the magnetic field parallel to the propagation direction of the standing wave and the level shift is

$$\Delta E_{\text{Zeeman}} = g_F \mu_B B m_F, \tag{17}$$

where  $g_F$  is the Landé factor,  $\mu_B$  is the Bohr magneton,  $B$  is the magnetic field intensity and  $m_F$  is the quantum number of the magnetic sub-level. The Zeeman-shifted sub-levels of the atomic ground state are again a.c. Stark shifted by an amount

$$\Delta E_{\text{a.c. Stark}} = \frac{\hbar \Delta \omega}{2} \left\{ \left[ 1 + \frac{f I(x) / I_{\text{sat}}(m_F)}{1 + 2(\Delta \omega / 2\beta)^2} \right]^{\frac{1}{2}} - 1 \right\}, \tag{18}$$

where the oscillator strength  $f$  and the saturation intensity  $I_{\text{sat}}(m_F)$  depend on the polarisation of the light and the particular  $m_F$  sublevel that is being excited (Ungar *et al.* 1989). Thus the total shift of an atomic ground state sub-level in a magnetic field and a blue-detuned and  $\sigma^-$  polarised standing wave is

$$\frac{\Delta E_{F, m_F}(x)}{\hbar} = \frac{g_F \mu_B B m_F}{\hbar} + \frac{\Delta \omega}{2} \left\{ \left[ 1 + \frac{f G(m_F) \cos^2 kx}{1 + 2(\Delta \omega / 2\beta)^2} \right]^{\frac{1}{2}} - 1 \right\}. \tag{19}$$

The a.c. Stark splitting of the magnetic sub-levels of the ground state  $2S_{1/2}, F = 2$  of sodium in a blue-detuned and  $\sigma^-$  polarised standing wave is shown in Fig. 16. Since in a blue-detuned and  $\sigma^-$  polarised standing wave, the sub-level with  $m_F = -2$  has the largest a.c. Stark shift and there is nearly no shift for the sub-level with  $m_F = 2$ , the sub-levels cross at several spatial points.

Now we consider the Sisyphus process for sub-Doppler cooling. An atom in a blue-detuned and  $\sigma^-$  polarised light field will tend to be optically pumped into the lowest-energy (most Stark-shifted) sub-level of ground states ( $^2S_{1/2}, F=2, m_F=-2$  in our case) according to the transition rules. First we consider a cold atom moving below the level-crossing point. When the atom moves from the bottom of the a.c. Stark shifted sub-level  $^2S_{1/2}, F=2, m_F=-2$  (near a node of the standing wave), it loses kinetic energy. In order to mix the sub-levels, a very weak perpendicular magnetic field is applied, as mentioned above. Thus near the level-crossing point, Larmor precession occurs and the population is redistributed. If the atom has an initial kinetic energy less than the potential energy corresponding to level-crossing point, it will come back to the node. During the motion of atoms between two adjacent level-crossing points, the atom is again optically pumped to the bottom energy level. Repeating the above process will result in energy loss and thus the atomic motion is damped. When the initial atomic kinetic energy is larger than the potential energy corresponding to the level-crossing point, then after the atomic population is redistributed near the level-crossing point, the atom will still move closely to the antinode and will be optically pumped to the sub-level  $^2S_{1/2}, F=2, m_F=-2$ . When the atoms move back towards the level-crossing point, the population is again redistributed. A detailed consideration shows that there is equilibrium between cooling and heating when the atoms have kinetic energy much larger than the potential energy corresponding to the level-crossing point. Therefore, the cooling can occur only for very slow atoms or very slow atoms can be channelled in a potential. Adiabatic decrease of the parallel magnetic field can realise further cooling. It is interesting that in a blue-detuned but  $\sigma^+$  polarised standing wave, only laser heating can occur because in this case, there is no level-crossing point.

In conclusion, in our model, sub-Doppler cooling can occur in a blue-detuned and  $\sigma^-$  polarised standing wave.

## 5. Basic Concept of Atom Optics

In this section, we first develop an approach to describe the atomic matter wave propagation in a light field and define an effective refractive index analogous to classical optics and then give a proposal for a Fabry–Perot interference filter with cold atoms. We also describe a preliminary experiment for building an atomic cavity that is a method for the injection of atoms into the atomic cavity mode. Several possibilities to realise an atomic cavity are also discussed in this section.

### (5a) Geometrical Optics Approximation of Atomic Motion in a Light Field

The description of wave propagation in atom optics is very similar to that in classical optics as a result of the formal analogy between the time-independent Schrödinger equation in quantum mechanics and the scalar Helmholtz equation in classical optics. Wave properties such as diffraction and interference can therefore occur when atoms are sent through microscopic mechanical structures or a light field (Carnal 1992). Different from the radiation force treatment of atomic motion in a light field (Kazantsev *et al.* 1990), where the atom is considered as a particle, atom optics deals with the atomic motion as particle–wave propagation in the ‘medium’. It is more interesting in atom optics to consider atomic wave

propagation in a 'light medium' instead of a dielectric medium in classical optics according to the formal analogy between the Schrödinger equation and the scalar Helmholtz equation. In a light medium, the effective refractive index is described by an atomic potential energy in the light field. Thus the analogous propagation behaviour of an atomic de Broglie wave to classical electromagnetic wave must satisfy the same fundamental principles, e.g. focus, reflection, refraction, etc.

The nonlinear phenomena can also occur for atomic wave propagation in a nonlinear light medium. For example, a long-range interatomic correlation due to photon exchange between atoms in the laser beam produces an atomic nonlinearity which can be exploited to generate an atomic soliton in the laser beam (Lenz *et al.* 1993; Zhang 1993; Zhang *et al.* 1994). The nonlinearity of a light medium can also lead to nonlinear phenomena analogous to those in nonlinear optics, or can be called nonlinear atom optics.

Atomic cavities (Kasevich *et al.* 1990; Balykin and Letokhov 1989; Wallis *et al.* 1992) are also important for atom optics because of their laser-like property. During the oscillation of atoms in an atomic cavity with appropriate mode-selective elements, a monochromatic and coherent atomic wave can be realised. By using a partially-transparent atomic mirror, the coherent atoms can be subtracted from the cavity and then used for an interference experiment. The atomic cavities can increase the degeneracy factors in one mode higher than one (Balykin and Letokhov 1989; Wallis *et al.* 1992), which are expected to be used in observing Bose-Einstein condensation (Greytak and Kleppner 1984).

It is therefore necessary to discuss the propagation of an atomic de Broglie wave in a light medium according to the analogy of the time-independent Schrödinger equation with the Helmholtz equation in classical optics. The light can be studied both by geometrical optics or by wave optics, and it has been verified that the wave equation can lead to the geometrical optics results when several approximations are made (Born and Wolf 1975). In the study of atom optics, similar analogies also occur, as mentioned above. Besides, the atom also behaves like a particle and a wave (Schiff 1968), and therefore the geometrical methods can be employed as well to deal with the atoms travelling through the 'light medium' (recently a quantum field theory of the interaction of ultracold atoms with a light wave was developed by Zhang and Walls 1994).

It is well known that atoms obey the Schrödinger equation, and in this subsection for simplicity we adopt the wave function for one atom to study the behaviour of the atomic beam transmission. Since the wave function can be regarded as the probabilistic amplitude of finding the atoms, this simplification seems appropriate. In the time-independent or stationary case, the Schrödinger equation is reduced to the Helmholtz equation (this is just the free atom case), i.e.

$$(\nabla^2 + k^2)\psi(\mathbf{x}) = 0, \quad (20)$$

where  $\psi$  is the atomic wave function and  $k$  is the wave vector which takes the value

$$k = \sqrt{2mE/\hbar^2}, \quad (21)$$

in which  $m$  is the mass of the atom and  $E$  the incident energy of the atom. When the external potential  $U(\mathbf{x})$  is introduced, the equation becomes

$$\nabla^2\psi(\mathbf{x}) + 2m[E - U(\mathbf{x})]/\hbar^2\psi = 0. \quad (22)$$

Equation (22) is generalised to

$$\nabla^2\psi + n^2k^2\psi = 0, \quad (23)$$

and the effective refractive index  $n$  is explicitly related to the potential as

$$n = 1 - U(\mathbf{x})/E. \quad (24)$$

Hence it can be shown that the effective refractive index is related to the potential produced by the laser light which is associated with the intensity of the laser and the detuning of the laser atom system, and the incident energy of the atom itself (here we regard the atomic beam to be monochromatic and so the energy of the atom can be viewed as constant). On the other hand, we note that the effective refractive index is the characteristic quantity of the 3D manifolds for the association with the metric, while the latter is the characteristic quantity of the geometry because of its determinable effect in the differential geometry (Eguchi *et al.* 1980). Hence one can establish the atom optics equation based on equations (23) and (24) which can, in analogy with classical optics, determine the motion of the atoms as particles in propagation through the light medium, at least in principle. As is well known the atom also behaves as a wave, i.e. a de Broglie matter wave with the wavelength

$$\lambda = h/p, \quad (25)$$

where  $h$  is Planck's constant,  $p$  is the momentum of the atom ( $p = mv$  and  $v$  is the atomic velocity). Therefore the wave effect also occurs and so a geometry covering the effect including the wave properties should be attained.

Earlier we established the basic equations which seem to apply to atom optics problems, where the effect on the atom by light has been equalised to that of the 'light medium' with the effective refractive index  $n$ . Besides, based on these quantities we are able to derive the trajectory equation of the atom during transmission and action. According to this similarity between atom transmission in a light medium and light transmission in a dielectric medium, it is reasonable to apply the techniques of classical optics to atom optics which also deals with the issues of propagation, diffraction, etc.

When corpuscular properties are under consideration, many analogies have been found between classical optics and atom optics, e.g. the reflection and refraction of the atom by an atomic mirror, which of course obeys the law of reflection and refraction as in classical optics. Based on this, we can manage to design different atom optical elements to realise reflection, refraction, focussing and aberration, etc. Also, in the paraxial approximation, we are allowed to give the matrix form of the atomic trajectory and hence the different elements for atom optics can have a proper matrix, just like classical optics, so as to provide more convenience in the atom-optics design.

Here we give some simple cases to show how geometrical atom optics deals with atomic motion (or propagation) in light media. The first case is the refraction of an atomic wave at the surface between two light media. In classical optics, refraction is a common phenomenon and occurs because Fermat's principle is obeyed. In atom optics, a similar phenomenon should occur. Consider a slow atomic beam incident in a rectangular travelling wave light field at an oblique angle  $\theta$ , analogous to light incident in a dielectric medium. In the radiation force scheme, for red-detuned light field, the dipole force (here we neglect spontaneous emission) pushes atoms to the higher intensity field, whereas for blue-detuned, the dipole pulls atoms from a higher intensity field. When the atoms enter the red-detuned travelling wave field, they are accelerated in the  $x$ -direction (perpendicular to the propagation direction of the light wave) by the dipole force near the 'surface' of the light medium. [Of course, the process must be adiabatic (Chen *et al.* 1992), as this condition is difficult to satisfy for fast atoms and suddenly-varying surfaces. In fact, for slow atoms the 'suddenly-varying surface' can still be considered as a slowly-varying medium near the surface of a light medium if we consider the width of the rectangular intensity light beam large enough.] In the  $z$ -direction (parallel to the propagation direction of the light wave), the atomic velocity is constant. Therefore the atomic beam is refracted close to the  $x$ -axis. In the light field, the atomic motion direction is constant because of the homogeneity of the light field intensity. The refraction angle can be calculated as follows: if the incident kinetic energy is  $E$  and incident angle is  $\theta_1$ , then after the action of the potential, the total kinetic energy becomes  $E' = E - U$  and the  $z$ -component of kinetic energy is constant, that is  $E_z = E \sin^2 \theta_1$ . The refraction angle is then obtained as  $\sin^2 \theta_2 = E \sin^2 \theta_1 / (E - U)$ , that is

$$\frac{\sin \theta_1}{\sin \theta_2} = \sqrt{1 - \frac{U}{E}} = n, \quad (26)$$

which is just the refraction law in geometrical optics. Therefore, geometrical atom optics gives a direct description of atomic motion in a light field.

Another interesting phenomenon is a possible atomic wave guide in a laser light beam. Assuming that the potential produced by light has a quadratic form, then the effective refractive index takes the form as (we assume that the problem is two-dimensional, i.e. the transverse is one dimension and  $z$  is the axis coordinate)

$$n = n_0 - \frac{1}{2}n_2^2x^2 \quad (n_2^2x^2 \ll n_0 \text{ the paraxial case}), \quad (27)$$

where  $n_0, n_2$  are both independent of the coordinate. Under the paraxial case, the trajectory equation becomes

$$\frac{d^2x}{dz^2} + n_2^2x = 0 \quad (28)$$

which has the solution

$$x(z) = \cos(n_2z)x_0 + n_2^{-1} \sin(n_2z)x'_0, \quad (29)$$

$$x'(z) = -n_2 \sin(n_2z)x_0 + \cos(n_2z)x'_0, \quad (30)$$

where the initial condition of the atomic beam is  $x|_{z=0} = x_0$  while  $dx/dz|_{z=0} = x'_0$ . We can evidently find that the atom takes a sinusoid trajectory in the light medium and hence it may be applied to produce an 'atomic wave fibre' to guide the motion of the atom, as well as the manipulation of the motion of the atom by the light if we can find a way to produce light with the potential to satisfy equation (27) (recently atomic waveguides from hollow optical fibres were proposed, see Marksteiner *et al.* 1994).

### (5b) Fabry-Perot Interference Filter with Cold Atoms

One aim is to further compress the velocity distribution of cold atoms, or optical molasses, which is useful for longitudinal mode selection of an atomic matter wave cavity (Balykin and Letokhov 1989; Wallis *et al.* 1992; Aminoff *et al.* 1993). By using the Raman velocity selection technique, Kasevitch and Chu (1992) obtained a velocity distribution with a width corresponding to 1/10 photon recoil kinetic energy in an optical molasses.

Here a simple method is proposed to select the velocity distribution of cold atoms by using a Fabry-Perot interference filter. The idea is based on an optical wavelength filter (Born and Wolf 1975).

Wilkens *et al.* (1993) proposed an Fabry-Perot interferometer for atoms. In their proposal, a double-humped potential is used for the interferometer scheme. But the small tunneling rate through the light potential practically limits the application as a wavelength filter for atoms. Here instead of a double-humped potential, we use a rectangular light potential well as a Fabry-Perot interference filter, which behaves like a solid etalon in classical optics. Consider slow atoms are normally incident to a rectangular laser light field (Xie *et al.* 1993) with a potential

$$U(x) = \begin{cases} 0 & x < 0 \text{ and } x > a, \\ U_0 & 0 < x < a. \end{cases} \quad (31)$$

For slow atoms,  $U_0$  is given by equation (16). For fast atoms, however, the potential is velocity-dependent and cannot be given in simple terms (Liu *et al.* 1994). In this paper, we consider only slow atoms which can be obtained from optical molasses (Metcalf and van der Straten 1994). The potential given by equation (31) leads to an effective refractive index

$$n(x) = \begin{cases} 1 & x < 0 \text{ and } x > a, \\ \sqrt{1 - U_0/E} = n_0 & 0 < x < a. \end{cases} \quad (32)$$

Equation (32) gives a rectangular profile of the reflective index imposed by a light medium. When slow atoms are normally the incident to this light medium, if the atomic incident kinetic energy is larger than the light field potential barrier or if the light field potential is a well, the transmission coefficient can be easily obtained from equation (22) as

$$T = \frac{4n_0^2}{(n_0^2 - 1)^2 \sin^2(n_0ka) + 4n_0^2} \quad \text{when } 0 < U_0 < E \text{ or } U_0 < 0. \quad (33)$$

Equation (33) is a periodic function. If we do not consider spontaneous emission for atoms in a light medium, which leads to loss of atom coherence (Pfau *et al.* 1994), the *peak-transmission*  $\tau$  for equation (33) is equal to unity. The perfect transmission occurs for

$$n_0ka = j\pi \quad (j = 1, 2, \dots). \quad (34)$$

The *contrast factor*  $\mathcal{E}$  for equation (33) is

$$\mathcal{E} = T_{\max}/T_{\min} = 1 + \frac{(n_0^2 - 1)^2}{4n_0^2}. \quad (35)$$

There are two ways to increase the contrast factor, one is to let  $n_0 \rightarrow 0$ , which means  $E \rightarrow U_0$ ; this case is very difficult to realise and to control. Another way to increase  $n_0$  is to increase the depth of the potential well, because in this case  $U_0 < 0$  and the effective refractive index is

$$n_0 = \sqrt{1 + |U_0|/E}. \quad (36)$$

If  $|U_0| \gg E$ , then  $n_0 \gg 1$  and the contrast factor  $\mathcal{E} \gg 1$ . Therefore a deep potential well is ideal for an atomic Fabry–Perot-type interference filter. It is easy to realise a potential well by negative detuning  $\Delta\omega$  according to equation (16). For an interference filter, it is interesting to know the free spectral range and the wavelength half-width, which is defined as the interval between wavelengths in the transmission band at which the transmission coefficient has fallen to half its maximum value. It is convenient to express the free spectral range and the wavelength half-width by a wave number change. In the approximation  $|U_0| \gg E$ , we have the finesse

$$\mathcal{F} = \frac{\pi}{4} \sqrt{\frac{|U_0|}{E}}, \quad (37)$$

the contrast factor

$$\mathcal{E} = \frac{1}{4} \frac{|U_0|}{E}, \quad (38)$$

the free-spectral range,

$$\Delta k_{fs} = \frac{\pi}{a} \sqrt{\frac{|U_0|}{E}} \quad \text{or} \quad \Delta v_{fs} = \frac{\pi\hbar}{ma} \sqrt{\frac{|U_0|}{E}}, \quad (39)$$

and the half-width

$$\Delta k_{hw} = \frac{8}{a} \quad \text{or} \quad \Delta v_{hw} = \frac{8\hbar}{ma}. \quad (40)$$

We have used  $k = mv/\hbar$ , where  $v$  is the atomic velocity. It is interesting to note that the half-width expressed in terms of atomic velocity is independent of the light potential and the kinetic energy when  $|U_0| \gg E$ . The half-width is determined only by the atomic mass and the width of the potential. To estimate the half-width and the free-spectral range, we consider a laser beam of width  $a = 1$  mm, and sodium atoms which have been cooled to 1/10 of the single photon recoil temperature in an optical molasses (Kasevich and Chu 1992), yielding a value of which  $E/\hbar = 0.54$  MHz. The laser has a detuning  $\Delta\omega/2\pi = 400$  MHz with respect to the sodium  $D_2$  transition and the on-resonance Rabi frequency of the laser is  $\Omega/2\pi = 400$  MHz. With these parameters we obtain from equation (16), the potential  $U_0/\hbar = -509.5$  MHz, or  $|U_0|/E = 943.5$ . Thus we have the half-width in velocity space

$$\Delta v_{hw} = 2.2 \times 10^{-3} \text{ cm s}^{-1}, \quad (41)$$

the free-spectral range

$$\Delta v_{fs} = 12.0 \Delta v_{hw} = 2.6 \times 10^{-2} \text{ cm s}^{-1}, \quad (42)$$

and the contrast factor

$$\mathcal{E} = 236. \quad (43)$$

Equation (41) describes an extremely narrow velocity distribution of atoms that are transmitted through the Fabry–Perot-type interference filter. Such a narrow distribution cannot be realised by present cooling techniques. With a free-spectral range given by equation (42), which is 12 times the half-width, and with a contrast factor as large as 236 given by equation (43), different modes can be easily distinguished. To realise single mode output, it is possible to use two or even more light fields with different refractive index or light field width, similar to the process of single mode selection in dye lasers. Since only a small fraction of atoms is transmitted through the Fabry–Perot interference filter, the brightness of the atomic wave will be small. It may be possible to use an atomic cavity to overcome this problem: continued injection of cold atoms into an atomic cavity with appropriate Fabry–Perot interference filters, or etalons can lead to single mode, coherent and bright atomic matter waves (Balykin and Letokhov 1989; Wallis *et al.* 1992; Aminoff *et al.* 1993).

Other possible applications of atomic interference in a light medium immediately come to mind. For example, similar to multilayer interference coatings in classical optics, an appropriate arrangement of multilayer light mediums makes possible an efficient reflection of the atomic matter wave. The use of two or more light medium layer coatings also makes possible a broader, lower-reflectance region with almost any specified matter wavelength-dependent transmittance. It is also possible to use multilayer interference coatings as a narrow band-pass filter to select atomic velocity of a thermal atomic beam. Other kinds of interference methods are also possible (Born and Wolf 1975).

In atomic interference spontaneous emission plays an important role. Spontaneous emission will damage the atomic coherence (Pfau *et al.* 1994) because of the stochastic process of momentum recoil of atoms. Therefore successful atomic

interference should avoid spontaneous emission and appropriate selection of laser light intensity and detuning is very important. It is also possible to study the influence of spontaneous emission on atomic interference by studying the damage of atomic interference due to spontaneous emission in Fabry–Perot-type interferometers.

### (5c) Injection of Atoms into an Atomic Cavity Mode

The atomic cavity was first considered by Balykin and Letokhov (1989) and a theoretical analysis was given by Wallis *et al.* (1992) for a single-mirror cavity which was realised by Aminof *et al.* (1993). One important factor in constructing an atomic cavity is the injection of atoms into the cavity mode. It is possible to eject atoms from a MOT, but this case leads to the following experiments to be discontinuous due to the filling time of the MOT. In contrast continuous injection of atoms can be realised by using laser cooled and compressed atomic beams (Scholz *et al.* 1994). Balykin and Letokhov also proposed a continuous atomic injection scheme based on laser collimation of an atomic beam (see Fig. 1a in Balykin and Letokhov 1989). For this purpose, a standing wave is introduced into the cavity so that its wave propagation direction is at right angles to the cavity axis. An atomic beam to be injected into the cavity mode at a slight angle  $\theta$  with respect to the cavity axis, here we call this angle the injection angle, is made to intersect the cavity axis at the same point as the standing wave. After the interaction with a blue-detuned standing wave, the atomic beam will be collimated in a direction perpendicular to the standing wave, i.e. in the direction of the cavity mode.

Here we report an preliminary experiment on a method for the injection of atoms into atomic cavity mode. The basic idea of our experiment follows Balykin and Letokhov's (1989) proposal and the configuration of the experimental scheme is shown in Fig. 17. The atomic beam, with most probable longitudinal velocity  $v_{mpl} = 500 \text{ m s}^{-1}$ , is collimated to  $\pm 1.5 \times 10^{-3}$  rad. A cw ring dye laser is used to irradiate an AOM with modulation frequency  $\Delta\omega$  to produce a zero-order light beam with frequency  $\omega_L$  and two first-order beams with frequency  $\omega_L \pm \Delta\omega$ . The atomic beam is irradiated in the interaction region by a blue-detuned standing wave, which propagates along the  $z$ -axis, while the atomic beam lies in the  $x$ - $z$  plane and is tilted at an oblique angle  $\theta$  with respect to the  $x$ -axis, which is also the cavity axis. We use a zero-order light beam with frequency  $\omega_L$  to irradiate the atomic beam in the interaction region. The final velocity profile is analysed by using the LIFM, described in Section 2b. One of the first-order light beams with frequency  $\omega_L - \Delta\omega$ , tuned to be strictly resonant with the  $D_2$  line of sodium, is used to induce fluorescence of atoms in the detection region located 0.7 m downstream from the interaction region. The interaction laser beam is tuned near the  $3S_{1/2}, F = 2 \rightarrow 3P_{3/2}, F = 3$  resonance transition of sodium atoms and is  $\sigma^+$  polarised (a weak dc magnetic field is applied along the  $z$ -axis) and, therefore, a two-level atomic system is achieved. The atomic oven is moved parallel to the propagation direction of the standing wave for obtaining different injection angles. For keeping the injection point of the atomic beam at the standing wave constant when moving the atomic oven, a collimation hole of diameter 0.8 mm is placed just in front of the interaction region. In the interaction region, the laser standing wave has a Gaussian profile with a beam waist  $w = 6$  mm.

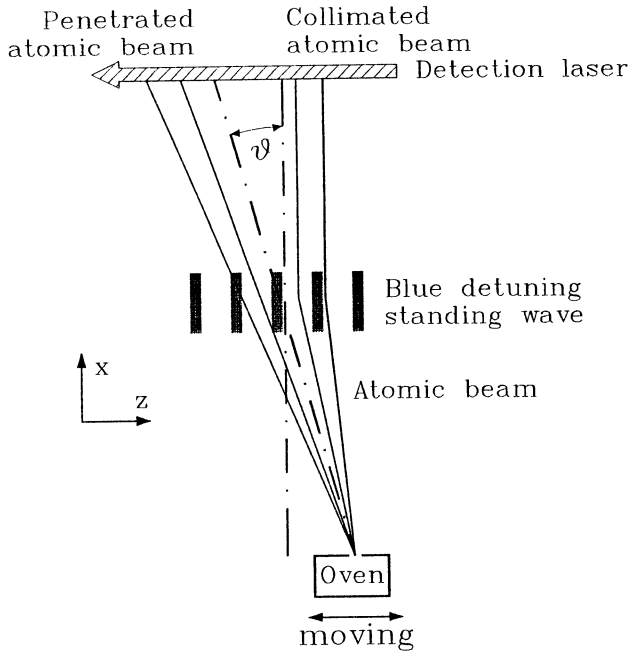
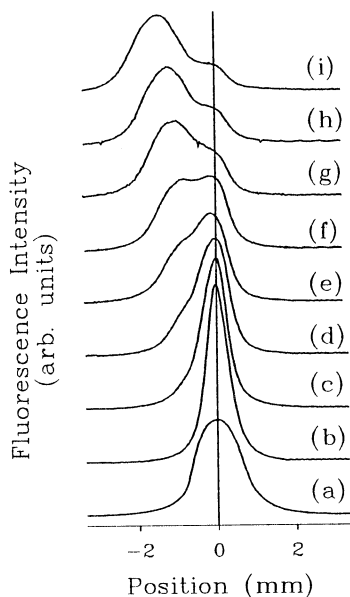


Fig. 17. Experimental scheme for the collimation of an atomic beam with an injection angle  $\theta$ .

Fig. 18 gives the experimental results for the collimation of an atomic beam in a blue-detuned standing wave with different injection angles. The cooling and collimation of the atomic beam by the stimulated force in a standing wave whose propagation direction is strictly perpendicular to the atomic beam is shown in Fig. 18*b* (Aspect *et al.* 1986; Wang *et al.* 1994*a*). With increasing the injection angle, part of the atomic beam is deflected and collimated by the standing wave and the rest goes in another direction. In other words, the atomic beam is split. These phenomena can be explained by the well-known theory of atomic motion in a standing wave (Minogin and Serimaa 1979; Dalibard and Cohen-Tannoudji 1985*b*; Liu and Wang 1991; Chen *et al.* 1993*a, b*). If the divergence angle of the atomic beam is  $2\eta$ , the transverse velocity parallel to the propagation direction of the standing wave is  $v_t = v_l \sin(\theta - \eta)$  (here  $\eta$  is zero at the centre of the atomic beam and  $\eta > 0$  when clockwise, otherwise  $\eta < 0$ ). From the theory, we know that there is a critical velocity. In a blue-detuned standing wave, atoms with velocity smaller than this critical velocity are cooled and otherwise heated. When  $\theta \sim 0$ , the transverse velocity  $v_t$  is determined by the divergence angle  $\eta$ . The atomic beam with  $\eta$  larger than the critical angle is heated and, with  $\eta$  smaller than the critical angle, the atomic beam is cooled to the zero transverse velocity or collimated (parallel to the propagation direction of the centre of the atomic beam where the transverse velocity is zero) (Aspect *et al.* 1986; Wang *et al.* 1994*a*), as shown in Fig. 18*b*. When the injection angle  $\theta$  is increased, the centre of the atomic beam also has a transverse velocity parallel to the propagation direction of the standing wave, and the transverse velocity of the atomic beam is larger for clockwise direction and smaller for anticlockwise. Therefore, the transverse velocity corresponding to the right-hand part of the atomic beam in

Fig. 17 is smaller than the left-hand part, and the left-hand part is heated and deflected to the left, but the right-hand part with small transverse velocity is cooled to zero velocity or collimated. Thus the atomic beam is split into two parts, the left-hand part is deflected to the left and has larger transverse velocity than the original one, and the right-hand part is cooled and collimated to zero transverse velocity. The channelling in a standing wave can also affect the above results (Salomon *et al.* 1987). The channelling of atoms in a standing wave occurs due to the so-called dipole force produced by the intensity gradient of the standing wave. We calculated the dipole force in detail (Liu *et al.* 1994) and found a space-phase retardation of the dipole force. The retardation depends on the atomic velocity and the dipole force can confine only slow atoms. For large velocity atoms, which correspond to the left-hand part of the atomic beam, they are not confined by the dipole force and penetrate the standing wave. When the atoms enter the standing wave with a low enough kinetic energy, they are guided into the channels where they oscillate in the transverse direction. The channelling takes place near the nodes if the detuning is positive and near the antinodes if the detuning is negative. When the slow atoms oscillate in the channels of the standing wave together with a weak dc magnetic field, we have demonstrated that the atoms will lose their kinetic energy, and sub-Doppler laser cooling can occur (Wang *et al.* 1990). This case means that a collimated atomic beam by stimulated force can be further collimated by the oscillation force below the Doppler limit.



**Fig. 18.** Experimental results for the collimation of an atomic beam by a blue-detuned standing wave with various injection angles (a) original profile of the atomic beam, (b)  $\theta = 0$ , (c)  $\theta = 4.4 \times 10^{-4}$ , (d)  $\theta = 8.9 \times 10^{-4}$ , (e)  $\theta = 1.3 \times 10^{-3}$ , (f)  $\theta = 1.8 \times 10^{-3}$ , (g)  $\theta = 2.2 \times 10^{-3}$ , (h)  $\theta = 2.7 \times 10^{-3}$ , (i)  $\theta = 3.1 \times 10^{-3}$  rad. The Rabi frequency of the standing wave is  $8.89\beta$  and the detuning is  $+10\beta$ .

In Fig. 18, an important phenomenon should be pointed out. When the injection angle  $\theta$  is changed, the collimated part of the atomic beam keeps the same position but the position of the penetrated part is changed. The collimated part can then be used as the injection of atoms into an atomic cavity. Fig. 18 also shows that the collimated atomic beam has a quite wide spatial profile

which does not mean that the atomic beam is not well collimated because the collimation corresponds to velocity space and all of the atoms in this part have a zero transverse velocity at a different position or they move parallel to each other in the direction which is strictly perpendicular to the propagation direction of the standing wave. In fact, this profile width comes from the different injection position of the atomic beam at the standing wave. For the injection angle  $\theta = 0$ , the transverse velocity is determined only by the divergence angle  $\eta$  in the interaction region and thus the cooling and collimation of the atomic beam leads to spatial profile compression, as shown in Fig. 18*b*. But when increasing the injection angle, the cooling and collimation occur at different positions in the standing wave, which leads to a width of the collimated atomic beam equal to the width of the atomic beam in the interaction region.

A simple calculation for the standing wave to trap the atomic velocity is necessary. Consider a typical case, as shown in Fig. 18*f*, where the collimated atomic beam has a width of 1.5 mm and the injection angle is  $1.8 \times 10^{-3}$  rad. Assuming the collimated atomic beam has the same width at the detection region as the interaction region, then the maximum velocity, which is also the critical velocity described above, trapped by the standing wave is about  $0.4 \text{ ms}^{-1}$ , which is in agreement with the theoretical prediction (Wang *et al.* 1994). From Fig. 18*f*, we find that nearly half the atomic beam is collimated. Increasing the injection angle leads to less atoms being collimated. This case can be easily understood as increasing the injection angle leads to a supplementary transverse velocity and then more atoms have transverse velocity larger than  $0.4 \text{ ms}^{-1}$ . Over this transverse velocity, the atoms will penetrate the standing wave. The trapping velocity increases when increasing the intensity and detuning of the standing wave (Liu and Wang 1991; Chen *et al.* 1993*a, b*; Wang *et al.* 1990; Salomon *et al.* 1987).

Our experimental results can be used in the atomic cavity proposed by Balykin and Letokhov (1989). In their proposal, the evanescent wave produced upon total internal reflection of a laser beam at a dielectric vacuum interface is used as an atomic cavity mirror (one of them should be curved for a stable oscillation mode, see Wallis *et al.* 1992 and Aminoff *et al.* 1993). The axis of the atomic cavity is perpendicular to two mirrors. We assume that the injected atoms are a three-level  $\Lambda$  system with two ground states  $|1\rangle$  and  $|2\rangle$  and one excited state  $|3\rangle$ . The collimation standing wave is blue-tuned around the transition between  $|2\rangle$  and  $|3\rangle$ . Consider a slow atomic beam (Scholz *et al.* 1994) with velocity  $30 \text{ ms}^{-1}$  injected into a standing wave with injection angle  $\sim 10^{-2}$ , then the transverse velocity corresponding to the standing wave is  $0.3 \text{ ms}^{-1}$  which is lower than the typical trapping velocity of the standing wave and all of the atomic beam can be collimated into the axis direction of the atomic cavity. The second standing wave is also tuned around the  $|2\rangle \rightarrow |3\rangle$  transition and pumps the atoms to another ground state  $|1\rangle$ , or prepares the atoms to the dark state for both standing waves. This standing wave is also used for further collimation of the atomic beam by using sub-Doppler transient laser cooling (Padua *et al.* 1993). It is obvious that this standing wave must be two-dimensional. The laser beam for producing the surface evanescent wave is tuned to the transition between  $|1\rangle$  and  $|3\rangle$  and thus the atoms are reflected by the atomic mirrors. In this configuration, the atoms oscillate in the cavity mode and during the oscillation, both standing

waves do not influence atoms in the atomic cavity mode. It is possible to use the Fabry–Perot interference filter, described in Section 5*b*, as a mode selector with which the velocity distribution (or spectral linewidth) can be extremely narrow. Continuous injection of atoms into the atomic cavity mode leads to atomic density in the mode high enough to satisfy the condition of Bose–Einstein condensation and thus Bose–Einstein condensation be experimentally observed (Metcalf 1994).

Obviously the linear atomic cavity can be extended to the circular one. The basic parameters of the atomic cavity can be found in Balykin and Letokhov (1989).

## 6. Conclusion and Discussion

We have presented an experimental investigation of atomic motion in a standing wave field, laser cooling in a diffuse light field, sub-Doppler cooling in a blue-detuned and  $\sigma^-$  polarised standing wave and given some concepts on atom optics and an experiment on a method for the injection of atoms into an atomic cavity mode.

The classical motion of atoms in a standing wave field, or radiation force on a two-level atom in a standing wave, has been extensively studied and the basic process is clear. It is possible to use this standing wave field force for further research or to build some elements, e.g. recently Li (1994) developed an atomic lens by using a dipole force in a standing wave and the scanning of an atomic beam by a standing wave. A misaligned standing wave supplies another parameter to control atomic motion, i.e. the misalignment angle. By changing the misalignment angle, it is easy to collimate or decollimate an atomic beam, instead of changing the laser power and frequency. Since the spatial wavelength of the misaligned standing wave is increased when increasing the misalignment angle, the long wavelength increases the region of linear velocity damping and then it is more efficient to longitudinally cool an atomic beam. When the atoms are channelled at the node or antinode of a misaligned standing wave, changing the misalignment angle leads to a change of wavelength and thus a change in distance among groups of channelled atoms. In other words, changing the misalignment angle can lead to a change in distance of the crystal lattice. This case is easily extended to a 3-D misaligned standing wave.

Laser longitudinal cooling of an atomic beam by a diffuse light field is a possible method to obtain cold atoms. If we use two or more integral spheres to increase the interaction distance and two or more lasers with different frequencies to adjust the lowest cooling velocity, the atoms can be cooled step by step to zero velocity. Compared with Zeeman tuning and frequency chirping, this method is simple and also efficient.

We first demonstrated that sub-Doppler laser cooling can occur in a blue-detuned standing wave. We developed a Sisyphus model to explain our sub-Doppler laser cooling, but the model is not complete. There is still a lot of theoretical and experimental work to be done on this model, e.g. in our model, an adiabatically decreasing magnetic field leads to further cooling, the sub-Doppler temperatures depending on the polarisation of the light field.

Recently atom optics has undergone great development. We have presented a description which is simple and clear but not complete. Since the light potential for atoms can be produced only when the light frequency is close to the atomic resonance transition frequency, it is necessary to consider atoms as a two- or

or multi-level system. We are trying to develop a new model to describe two-level atomic motion in a light field, which is called the vector model, compared with the description in Section 5. The vector model is more analogous to classical optics, e.g. birefringence can occur. Spontaneous emission has to be considered in the model except for some special cases. Spontaneous emission leads to a stochastic process in the propagation of the atomic matter wave (Wang *et al.* 1985) or dephase. This process strongly influences atomic interference and to study this process is valuable for building an atom interferometer. We also discussed the possibility of using a light field as a frequency filter for atoms, which can be used as a mode selector in an atomic cavity. We also reported a preliminary experiment on a method for the injection of atoms into an atomic cavity mode and discussed a possible atomic cavity.

### Acknowledgments

The authors would like to thank Prof. W. Q. Cai, Prof. R. F. Zhou, Dr X. Z. Chen, Mrs X. J. Wang, Mr H. X. Chen, Mr S. W. Fang for their efforts in the experiments and Mrs S. Y. Zhou and Mrs Y. S. Liu for their technical help. The authors also would like to thank Dr H. Guo and Prof. X. M. Deng for their cooperation in the theoretical work on atom optics and many stimulating discussions. Part of this manuscript was finished in the University of Kaiserslautern. L. L. warmly thanks Prof. K. Bergmann and members of the Graduierten Kolleg 'Laser und Teilchenspektroskopie' at the University of Kaiserslautern for their helpful discussions. This work was supported by the National Science Foundation of China.

### References

- Adams, C. S., Sigel, M., and Mlynek, J. (1994). *Phys. Rep.* **240**, 143.
- Aminoff, C. G., Steane, A. M., Bouyer, P., Desbiolles, P., Dalibard, J., and Cohen-Tannoudji, C. (1993). *Phys. Rev. Lett.* **71**, 3083.
- Andreev, S. V., Balykin, V. I., Letokhov, V. S., and Minogin, V. G. (1981). *Pis'ma Zh. Eksp. Teor. Fiz.* **34**, 463 [(1981). *JETP Lett.* **34**, 442].
- Ashkin, A. (1970). *Phys. Rev. Lett.* **25**, 1312.
- Ashkin, A. (1978). *Phys. Rev. Lett.* **40**, 729.
- Aspect, A., Dalibard, J., Heidmann, A., Salomon, C., and Cohen-Tannoudji, C. (1986). *Phys. Rev. Lett.* **57**, 1688.
- Aspect, A., Arimondo, E., Kaiser, R., Vansteenkiste, N., and Cohen-Tannoudji, C. (1988). *Phys. Rev. Lett.* **61**, 826.
- Aspect, A., Arimondo, E., Kaiser, R., Vansteenkiste, N., and Cohen-Tannoudji, C. (1989). *J. Opt. Soc. Am. B* **6**, 2112.
- Balykin, V. I. (1980). *Opt. Commun.* **33**, 31.
- Balykin, V. I., Letokhov, V. S., and Mushin, V. I. (1979). *Pis'ma Zh. Eksp. Teor. Fiz.* **29**, 614 [(1979). *JETP Lett.* **29**, 560].
- Balykin, V. I., Letokhov, V. S., and Mushin, V. I. (1980). *Zh. Eksp. Teor. Fiz.* **78**, 1367 [(1980). *Sov. Phys. JETP* **51**, 692].
- Balykin, V. I., Letokhov, V. S., and Sidorov, A. I. (1984a). *Opt. Commun.* **49**, 248.
- Balykin, V. I., Letokhov, V. S., and Sidorov, A. I. (1984b). *Zh. Eksp. Teor. Fiz.* **86**, 2019.
- Balykin, V. I., Letokhov, V. S., Ovchinnikov, Yu. B., and Sidorov, A. I. (1988). *Phys. Rev. Lett.* **60**, 2137.
- Balykin, V. I., and Letokhov, V. S. (1989). *Appl. Phys. B* **48**, 517.
- Balykin, V. I., Carnal, O., Heine, C., Pfau, T., Seifert, W., Sleator, T., and Mlynek, J. (1993). In 'Laser Spectroscopy XI' (Eds L. Bloomfield *et al.*), p. 79 (AIP Press: New York.)

- Batelaan, H., Padua, S., Yang, D. H., Xie, C., Gupta, R., and Metcalf, H. (1994). *Phys. Rev. A* **49**, 2780.
- Bjorkholm, J. E., Freeman, R. R., and Pearson, D. B. (1981). *Phys. Rev. A* **23**, 491.
- Blatt, R., Ertmer, W., and Hall, J. L. (1984). *Prog. Quantum Electron.* **8**, 119.
- Born, M., and Wolf, E. (1975). 'Principles of Optics' (Pergamon, Oxford).
- Breeden, T., and Metcalf, H. (1981). *Phys. Rev. Lett.* **47**, 1726.
- Carnal, O. (1992). Ph.D. Thesis, Swiss Federal Institute of Technology, Zürich.
- Carnal, O., and Mlynek, J. (1991). *Phys. Rev. Lett.* **66**, 2689.
- Castin, Y., Wallis, H., and Dalibard, J. (1989). *J. Opt. Soc. Am.* **6**, 2046.
- Chen, H. X., Liu, L., and Wang, Y. Z. (1994). *Acta Optica Sinica* **14**, 125.
- Chen, J., Sory, J. G., Tollett, J. J., and Hulet, R. G. (1992a). *Phys. Rev. Lett.* **69**, 1344.
- Chen, X. Z., Liu, L., and Wang, Y. Z. (1993a). *Acta Physica Sinica* **42**, 1587.
- Chen, X. Z., Liu, L., and Wang, Y. Z. (1993b). *Acta Optica Sinica* **13**, 1083.
- Chen, X. Z., Wang, X. J., Li, Z., Cai, W. Q., and Wang, Y. Z. (1992b). *Chinese J. Lasers (E.E.)* **1**, 509.
- Chu, S., Hollberg, L., Bjorkholm, J., Cable, A., and Ashkin, A. (1985). *Phys. Rev. Lett.* **55**, 48.
- Chu, S., Prentiss, M. G., Cable, A., and Bjorkholm, J. E. (1988). In 'Laser Spectroscopy VIII' (Eds W. Persson and S. Svanberg), p. 58 (Springer: Berlin).
- Cook, R. J., and Hill, R. K. (1982). *Opt. Commun.* **43**, 258.
- Dalibard, J., and Cohen-Tannoudji, C. (1985a). *J. Phys. B* **18**, 1661.
- Dalibard, J., and Cohen-Tannoudji, C. (1985b). *J. Opt. Soc. Am. B* **2**, 1707.
- Dalibard, J., and Cohen-Tannoudji, C. (1989). *J. Opt. Soc. Am. B* **6**, 2023.
- DeVoe, R. G. (1991). *Opt. Lett.* **16**, 1605.
- Eguchi, T., Gilky, P. B., and Hanson, A. J. (1980). *Phys. Rep.* **66**, 241.
- Einstein, A. (1916). *Mitt. Phys. Ges. (Zürich)* **18**, 47; (1917). *Physikalische Zeitschrift* **18**, 121.
- Ertmer, W., Blatt, R., Hall, J., and Zhu, M. (1985). *Phys. Rev. Lett.* **54**, 996.
- Esslinger, T., Weidemüller, M., Hemmerich, A., and Hänsch, T. (1993). *Opt. Lett.* **18**, 450.
- Frisch, O. R. (1933). *Z. Phys.* **86**, 42.
- Gallatin, G. M., and Gould, P. L. (1991). *J. Opt. Soc. Am. B* **8**, 502.
- Gordon, J. P., and Ashkin, A. (1980). *Phys. Rev. A* **21**, 1606.
- Gould, P. L., Ruff, G. A., and Pritchard, D. E. (1986). *Phys. Rev. Lett.* **56**, 827.
- Gozzini, S., Paffuti, G., Zuppini, D., Gabbanini, C., Moi, L., and Nienhuis, G. (1991). *Phys. Rev. A* **43**, 5005.
- Greytak, T. J., and Kleppner, D. (1984). In 'New Trends in Atomic Physics' (Eds G. Grynberg and R. Stora), p. 1125 (North Holland: Amsterdam).
- Guo, H., Liu, L., Wang, Y. Z., and Deng, X. M. (1994). 'Quasi-Geometrical Description of Atomic Motion in Light Field', *Phys. Rev. A*, submitted.
- Gupta, R., Xie, C., Padua, S., Batelaan, H., and Metcalf, H. (1993). *Phys. Rev. Lett.* **71**, 19.
- Hänsch, T. W., and Schawlow, A. L. (1975). *Opt. Commun.* **13**, 68.
- Hoffnagle, J. (1988). *Opt. Lett.* **13**, 102.
- Jaduszliwer, B., Dang, R., Weiss, P., and Bederson, B. (1980). *Phys. Rev. A* **21**, 808.
- Kasevich, M., and Chu, S. (1991b). *Phys. Rev. Lett.* **67**, 181.
- Kasevich, M., and Chu, S. (1992). *Phys. Rev. Lett.* **69**, 1741.
- Kasevich, M., Weiss, D., and Chu, S. (1990). *Opt. Lett.* **15**, 607.
- Kasevich, M., Weiss, D. S., Riis, E., Moler, K., Kasapi, S., and Chu, S. (1991a). *Phys. Rev. Lett.* **66**, 2297.
- Kazantsev, A. P., Smirnov, V. S., Surdutovich, G. I., Chudesnikov, D. O., and Yakovlev, V. P. (1985). *J. Opt. Soc. Am. B* **2**, 1731.
- Keith, D. W., Ekstrom, C. R., Turchette, Q. A., and Pritchard, D. E. (1991). *Phys. Rev. Lett.* **66**, 2693.
- Ketterle, W., Martin, A., Joffe, M. A., and Pritchard, D. E. (1992). *Phys. Rev. Lett.* **69**, 2483.
- Lebedev, P. N. (1910). *Ann. Phys. (Leipzig)* **32**, 411.
- Lenz, G., Meystre, P., and Wright, E. M. (1993). *Phys. Rev. Lett.* **71**, 3271.
- Letokhov, V. S., and Minogin, V. G. (1981). *Phys. Rep.* **73**, 1.
- Letokhov, V. S., Minogin, V. G., and Pavlik, B. D. (1977). *Zh. Eksp. Teor. Fiz.* **72**, 1328.
- Lett, P. D., Watts, R. N., Westbrook, C. I., Phillips, W. D., Gould, P. L., and Metcalf, H. J. (1988). *Phys. Rev. Lett.* **61**, 169.

- Lett, P. D., Phillips, W. D., Rolston, S. L., Tanner, C. E., Watts, R. N., and Westbrook, C. I. (1989). *J. Opt. Soc. Am.* **6**, 2084.
- Li, Q. (1994). Ph.D. Thesis, Australian National University.
- Liang, J., Moi, L., and Fabre, C. (1984). *Opt. Commun.* **52**, 131.
- Liu, L., and Wang, Y. Z. (1993). *Chinese J. Lasers (E.E.)* **B 2**, 11.
- Liu, L., Chen, H. X., and Wang, Y. Z. (1993). *Acta Physica Sinica* **42**, 1762.
- Liu, L., and Wang, Y. Z. (1991). *Acta Optica Sinica* **11**, 577.
- Liu, L., Chen, H. X., Li, F. S., and Wang, Y. Z. (1994). *Acta Optica Sinica*, Dipole Force with Retarded Phase in a Standing Wave, to be published.
- McClelland, J. J., and Scheinfein, M. R. (1991). *J. Opt. Soc. Am.* **B 8**, 1974.
- Marksteiner, S., Savage, C. M., Zoller, P., and Rolston, S. L. (1994). *Phys. Rev. A* **50**, 2680.
- Martin, P. J., Gould, P. L., Oldaker, B. G., Miklich, A. H., and Pritchard, D. E. (1987). *Phys. Rev. Lett.* **36**, 2459.
- Metcalf, H. (1994). personal communication.
- Metcalf, H., and van der Straten, P. (1994). *Phys. Rep.* **244**, 203.
- Migdall, A. L., Prodan, J. V., Phillips, W. D., Bergeman, T. H., and Metcalf, H. J. (1985). *Phys. Rev. Lett.* **54**, 2596.
- Minogin, V. G., and Serimaa, O. T. (1979). *Opt. Commun.* **30**, 373.
- Mlynek, J., Balykin, V., and Meystre, P. (Eds) (1992). *Appl. Phys. B* **54**, 319, 'Optics and Interferometry with Atoms', Special Issue.
- Moi, L. (1984). *Opt. Commun.* **50**, 349.
- Monroe, C., Swann, W., Robinson, H., and Wieman, C. (1990). *Phys. Rev. Lett.* **65**, 1571.
- Padua, S., Xie, C., Gupta, R., Batelaan, H., Bergeman, T., and Metcalf, H. (1993). *Phys. Rev. Lett.* **70**, 3217.
- Pfau, T., Spälter, S., Kurtsiefer, Ch., Ekstrom, C. R., and Mlynek, J. (1994). *Phys. Rev. Lett.* **73**, 1223.
- Phillips, W. D., and Metcalf, H. (1982). *Phys. Rev. Lett.* **48**, 596.
- Phillips, W. D., Prodan, J. V., and Metcalf, H. (1985). *J. Opt. Soc. Am.* **B 2**, 1751.
- Pillet, P. (Ed.) (1994). *J. de Phys. (France)* **4**, 1877, 'Optics and Interferometry with Atoms', Special Issue.
- Prodan, J. V., Phillips, W. D., and Metcalf, H. (1982). *Phys. Rev. Lett.* **49**, 1149.
- Prodan, J. V., Phillips, W. D., So, I., Metcalf, H., and Dalibard, J. (1985). *Phys. Rev. Lett.* **54**, 992.
- Raab, E., Prentiss, M., Cable, A., Chu, S., and Pritchard, D. (1987). *Phys. Rev. Lett.* **59**, 2613.
- Riehle, F., Kisters, Th., Witte, A., and Helmcke, J. (1991). *Phys. Rev. Lett.* **67**, 177.
- Salomon, C., Dalibard, J., Aspect, A., Metcalf, H., and Cohen-Tannoudji, C. (1987). *Phys. Rev. Lett.* **59**, 1659.
- Schieder, R., Walther, H., and Woste, L. (1972) *Opt. Commun.* **5**, 337.
- Schiff, I. I. (1968). 'Quantum Mechanics' (McGraw-Hill: New York.)
- Scholz, A., Christ, M., Doll, D., Ludwig, J., and Ertmer, W. (1994) *Opt. Commun.* **111**, 155.
- Shang, S.-Q., Sheehy, B., Straten, P. van der, and Metcalf, H. (1990). *Phys. Rev. Lett.* **65**, 317.
- Sheehy, B., Shang, S.-Q., Straten, P. van der, Hatamian, S., and Metcalf, H. (1990). *Phys. Rev. Lett.* **64**, 858.
- Sleator, T., Pfau, T., Balykin, V., and Mlynek, J. (1992a). *Appl. Phys. B* **54**, 375.
- Sleator, T., Pfau, T., Balykin, V., Carnal, O., and Mlynek, J. (1992b). *Phys. Rev. Lett.* **68**, 1996.
- Stenholm, S., Minogin, V. G., and Letokhov, V. S. (1978). *Opt. Commun.* **25**, 107.
- Straten, P. van der, Shang, S.-Q., Sheehy, B., and Metcalf, H. (1993). *Phys. Rev. A* **47**, 4160.
- Strohmeier, P., Kerseboom, T., Krüger, E., Nölle, H., Steuter, B., Schmand, J., and Andrä, J. (1989). *Opt. Commun.* **73**, 451.
- Umezu, J., and Shimizu, F. (1985). *Japanese J. Appl. Phys.* **24**, 1655.
- Ungar, P. J., Weiss, D. S., Riis, E., and Chu, S. (1989). *J. Opt. Soc. Am.* **B 6**, 2058.
- Wallis, H., Dalibard, J., and Cohen-Tannoudji, C. (1992). *Appl. Phys. B* **54**, 407.
- Wang, Y. Z. (1980). *Kexue Tongbao* **9**, 432; (1981). *Chinese J. Lasers* **8**, 10.
- Wang, Y. Z., Zhou, R. F., Zhou, Z. Y., Ni, G. Q., Zhou, S. Y., Wang, C. S., and Zheng, W. J. (1984a). *Scientia Sinica* **A 5**, 467.

- Wang, Y. Z., Zhou, R. F., Zhou, Z. Y., Ni, G. Q., and Cai, W. Q. (1984*b*). *Opt. Lett.* **9**, 276.
- Wang, Y. Z., Cheng, Y. D., Zhou, S. Y., Huang, W. G., and Liu, L. (1985). *Chinese J. Lasers* **12**, 658.
- Wang, Y. Z., Cheng, Y. D., Cai, W. Q., Wu, Y. S., Luo, Y., and Zhang, X. D. (1989). In 'Laser Spectroscopy IX' (Eds M. S. Feld, and J. E. Thomas), p. 455 (Academic: New York).
- Wang, Y. Z., Cai, W. Q., Cheng, Y. D., Liu, L., Luo, Y., and Zhang, X. D. (1990). *Phys. Rev. A* **42**, 4032.
- Wang, Y. Z., Ye, C., Wu, Y., Wang, X., Zhou, S., Cheng, Y., Ma, L., and Ding, L. (1993). *Chinese Phys. Lett.* **10**, 213.
- Wang, X. J., Liu, L., Chen, X. Z., Fang, S. W., and Wang, Y. Z. (1994*a*). *Acta Optica Sinica* **14**, 1161.
- Wang, Y. Z., Liu, L., Wang, X. J., Chen, X. Z., Fang, S. W., Cai, W. Q., Zhou, S. Y., and Liu, Y. S. (1994*b*). *Appl. Phys. B* **58**, 327.
- Weiss, D. S., Riis, E., Shevy, Y., Ungar, P. J., and Chu, S. (1989). *J. Opt. Soc. Am. B* **6**, 2072.
- Wilkens, M., Goldstein, E., Taylor, B., and Meystre, P. (1993). *Phys. Rev. A* **47**, 2366.
- Wineland, D., and Dehmelt, H. (1975). *Bull. Am. Phys. Soc.* **20**, 637.
- Wineland, D., and Itano, W. (1979). *Phys. Rev. A* **20**, 1521.
- Xie, C., Gupta, R., and Metcalf, H. (1993). *Opt. Lett.* **18**, 173.
- Zhang, W. (1993). *Phys. Lett. A* **176**, 225.
- Zhang, W., Walls, D. F., and Sanders, B. C. (1994). *Phys. Rev. Lett.* **72**, 60.
- Zhang, W., and Walls, D. F. (1994). *Phys. Rev. A* **49**, 3799.
- Zhu, M., Oates, C. W., and Hall, J. L. (1991). *Phys. Rev. Lett.* **67**, 46.
- Zueva, T. V., and Minogin, V. G. (1981). *Sov. Tech. Phys. Lett.* **7**, 411.

